UNIVERSITY OF NAPLES FEDERICO II

PH.D. PROGRAM IN

CLINICAL AND EXPERIMENTAL MEDICINE

CURRICULUM IN TRANSLATIONAL PEDIATRIC SCIENCES

XXXIII Cycle
(Years 2018-2021)

Chairman: Prof. Francesco Beguinot

PH.D. THESIS

TITLE

ALTERED BRAIN NETWORKS IN RETT SYNDROME: NEUROPHYSIOLOGICAL SIGNATURES

TUTOR

Prof. Carmela Bravaccio

PH.D. STUDENT

Dr. Pia Bernardo

Abstract

Introduction

1. Clinical symptoms
2. Genetic Background
3. Therapeutic Approaches
4. Neurophysiological Studies and Synaptic Plasticity

Clinical Setting: Neurophysiological Signatures of Motor Impairment in Patients with Rett Syndrome

1. Introduction
2. Methods
3. Results
4. Discussion

Clinical Setting: A Magnetoencephalographic Study of Network Connectivity in patients with Rett Syndrome

1. Introduction
2. Methods
3. Results
4. Discussion

Future perspectives: Validation of a new neurophysiological biomarker of motor disability in patients with Rett Syndrome: an innovative combined neurophysiology and physical therapy protocol to enhance cortical plasticity

Abstract

Objective: Rett syndrome (RTT) is an X-linked dominant neurodevelopmental disorder due to pathogenic mutations in the MECP2 gene. Motor impairment constitutes the core diagnostic feature of RTT. Preclinical studies have consistently demonstrated alteration of excitation/inhibition (E/I) balance and aberrant synaptic plasticity at the cortical level. We aimed to understand neurobiological mechanisms underlying motor deficit by assessing in vivo synaptic plasticity and E/I balance in the primary motor cortex (M1).

Methods: In the first work, we included 14 patients with typical RTT, 9 epilepsy control patients, and 11 healthy controls, we applied paired-pulse transcranial magnetic stimulation (TMS) protocols to evaluate the excitation index, a biomarker reflecting the contribution of inhibitory and facilitatory circuits in M1. Intermittent TMS-theta burst stimulation was used to probe long-term potentiation (LTP)-like plasticity in M1. Motor impairment, assessed by *ad hoc* clinical scales, was correlated with neurophysiological metrics. In the second study, we have studied 10 girls with RTT, using magnetoencephalography (MEG), based our analyses on source-reconstructed MEG data acquired during resting state.

Results: RTT patients displayed a significant increase of the excitation index ($p = 0.003$), as demonstrated by the reduction of short-interval intracortical inhibition and increase of intracortical facilitation, suggesting a shift toward cortical excitation likely due to GABAergic dysfunction. Impairment of inhibitory circuits was also confirmed by the reduction of long-interval intracortical inhibition ($p = 0.002$). LTP-like plasticity in M1 was abolished ($p = 0.008$) and scaled with motor disability (all $p = 0.003$). In addition, the MEG data suggested an alteration of brain connectivity.

Interpretation: To the best of our knowledge, this is the first study showing abnormalities of the E/I balance and synaptic plasticity in humans with RTT. These alterations were associated with a greater degree of functional motor disabilities, suggesting a pathophysiologic role of these functional changes. TMS is a method that can be used to assess cortical motor function in RTT patients. Our findings support the introduction of TMS measures in clinical and research settings to monitor the progression of motor deficit and response to treatment.

Introduction

Rett syndrome (RTT) is a rare genetic neurological disorder, first identified by Dr Andreas Rett in 1966, after he observed 22 patients with similar unique symptoms **[1]**. Bengt Hagberg and colleagues characterized the specific clinical features, defining RTT as a specific neurodevelopmental disorder **[2]**. In 1999, Amir and colleagues discovered genetic basis of RTT to be mutation in the gene encoding Methyl-CpG-binding protein 2 (MECP2), that are associated both with rare familial cases of RTT as well as with the more common sporadic occurrences of typical RTT **[3]**. Mutations in MECP2 can be found in 95–97% of individuals with typical RTT. Some years earlier, Dr Bird and colleagues **[4]** identified MeCP2 as a novel protein that binds to methylated CpG dinucleotides within the mammalian genome. This gene is involved in mechanisms of chromatin structure formation, and appears to regulate gene expression through the silencing or activation of other specific genes **[5, 6, 7]**. MECP2 is located on the X chromosome, Xq28 **[8]**, for this RTT is a disease that is almost exclusively seen in females. For the monogenic characteristic of RTT, some Mecp2 knockout models have been generated in mice **[9, 10, 11, 12, 13]**. To date, animal studies are a source of important information on the neurological and psychiatric characteristics of the disease, as well as a model for experiments on drug treatments

1. Clinical symptoms

RTT is a primary cause of intellectual disability in girls, after Down syndrome, with an incidence of 1 in 10,000 female births **[14]**. RTT is a predominantly neurodevelopmental disorder, which evolves with progressive symptoms, which manifest themselves over the years, classically divided into different stages. The first point is that subjects with RTT appear to develop normally up to 6–18 months of age, followed by regression of psychomotor development as motor function and social communication skills. In the past, the decelerate growth of the head circumference of Rett girl was the key for diagnosis **[15].** Later, Neul et al **[14]** eliminated post-natal deceleration in head growth from the necessary criteria because this feature in not found in all individuals with typical RTT. However, because it is a clinical feature that can alert a clinician to the potential diagnosis and it is a distinctive feature in the disorder, the authors included this as a preamble to the criteria as a feature that should raise suspicion for the diagnosis. Distinctive aspects contributing to the diagnosis include developmental regression, with accompanying loss of hand skills, mobility skills, and speech and typical stereotypic hand movements. As the syndrome progresses, social and language skills become apparent with features reminiscent of autism spectrum disorder **[16]**. The onset of cognitive deterioration is accompanied by loss of motor abilities and the development of ataxia and gait apraxia. Microcephaly, respiratory and autonomic disfunctions **[17]**, epilepsy, sleep disorders, scoliosis, growth deficits and early hypotonia are very prevalent. Epilepsy is frequent, with a percentage ranging from 60 to 80% of cases, with an onset after 3 years. the percentage of drug resistance is 30% **[18]**. Interesting, neurophysiologic evaluations show cortical hyperexcitability on the electroencephalogram (EEG), which represents a loss of expected developmental features and the occurrence of rhythmic slow activity, primarily in the frontal-central regions **[18]**. However, the diagnosis can be tricky due to the presence of many other movement and behavioral disorders that may be present, including teeth grinding, night laughing or crying, screaming fits, low mood, and anxiety episodes elicited by distressing external events **[19]**.

Most girls with RTT lose mobility and are often wheelchair-bound during the teenage years. Impairment of the autonomic nervous system in RTT is suggested by an increased incidence of long Q–T intervals during electrocardiographic recordings and it can contribute to the higher incidence rate of sudden unexpected death in RTT patients. Other autonomic abnormalities include

hypotrophic cold blue feet; severe constipation; oropharyngeal dysfunction; and cardiac abnormalities, including tachycardia and sinus bradycardia. Even with high risk of sudden death because of respiratory and cardiac dysfunctions, several patients survive till the 6th or 7th decade of life with limited mobility **[20]**.

To address some of the confusion that currently exists regarding the diagnosis of RTT, the RettSearch Consortium participated in an iterative process to come to a consensus on revised and simplified diagnostic criteria for RTT. The previous criteria of 2002 had eight necessary criteria, five exclusion criteria, and eight supportive criteria. The requirement for those criteria was never explicitly stated and one of the necessary criteria (postnatal deceleration of head growth in majority) was not absolutely required; furthermore, there was no requirement for any of the supportive criteria. Neul et al. **[14]** developed revised diagnostic criteria (**Table 1**) to clarify and simplify the diagnosis of typical, or classic, RTT. We limited the necessary criteria to the presence of regression plus four main criteria that are absolutely required for the diagnosis of typical RTT.

Table 1

Revised diagnostic criteria for RTT.

RTT Diagnostic Criteria 2010	
Consider diagnosis when postnatal deceleration of head growth observed.	
Required for typical or classic RTT	
1	A period of regression followed by recovery or stabilization*
2	All main criteria and all exclusion criteria
3	Supportive criteria are not required, although often present in typical RTT
Required for atypical or variant RTT	
1	A period of regression followed by recovery or stabilization*
2	At least 2 out of the 4 main criteria
3	5 out of 11 supportive criteria
Main Criteria	
1	Partial or complete loss of acquired purposeful hand skills.
2	Partial or complete loss of acquired spoken language**
3	Gait abnormalities: Impaired (dyspraxic) or absence of ability.
4	Stereotypic hand movements such as hand wringing/squeezing, clapping/tapping, mouthing and washing/rubbing automatisms
Exclusion Criteria for typical RTT	
1	Brain injury secondary to trauma (peri- or postnatally), neurometabolic disease, or severe infection that causes neurological problems***
2	Grossly abnormal psychomotor development in first 6 months of life#
Supportive Criteria for atypical RTT##	
1	Breathing disturbances when awake
2	Bruxism when awake
3	Impaired sleep pattern
4	Abnormal muscle tone
5	Peripheral vasomotor disturbances
6	Scoliosis/kyphosis
7	Growth retardation
8	Small cold hands and feet
9	Inappropriate laughing/screaming spells
10	Diminished response to pain
11	Intense eye communication - "eye pointing"

The differential diagnosis is made with the so-called Rett-like disorders, which present symptoms and signs similar to the typical Rett syndrome MECP2-related. The term Rett-like refers to phenotypes with distinct overlapping features of Rett syndrome where the clinical criteria are not completely fulfilled. The differential diagnostics in Rett syndrome has evolved with the development of next generation sequencing-based techniques and many patients have been

diagnosed with other syndromes or variants in newly described genes where the associated phenotype(s) is yet to be fully explored.

Differential Diagnosis Disorder	Gene(s)/Genetic Mechanism	Overlapping w/MECP2 Disorders	Distinguishing from MECP2 Disorders
Angelman syndrome	Deficient expression or function of maternally inherited UBE3A allele	ID, severe speech impairment, gait ataxia &/or tremulousness of the limbs; microcephaly & seizures common; DD 1st noted at age ~6 mos	In classic Rett syndrome DD is not overtly evident in the 1st 6 mos.
Early infantile epileptic encephalopathy (OMIM 300672)	CDKL5	In females: early-onset severe seizures w/poor cognitive development; facial gestalt, cortical visual impairment; In males: severe-profound ID & early-onset intractable seizures 2	Very early-onset seizures, facial dysmorphism, & cortical visual impairment are not generally seen in classic Rett syndrome.
Rett syndrome, congenital variant (OMIM 613454)	FOXG1	Short normal period of development before onset of regression leading to severe ID, DD, postnatal microcephaly, agenesis of the corpus callosum, seizures, dyskinesia, & hypotonia 3	Except for microcephaly, structural abnormalities are not usually seen on brain MRI.

To date, several laboratories have available gene panels that allow the search for multiple genes at the same time when the patient presents symptoms attributable to the RTT.

PANNELLO MULTIGENICO

DISABILITA' INTELLETTIVA/DISTURBI DELLO SPETTRO AUTISTICO

ADNP, ANKRD11, AP1S2, ARFGEF2, ARID1B, ARX, ASH1L, ATRX, CASK, CC2D1A, CDKL5, CHD8, CNTNAP2, CREBBP, CTNNB1, DEAF1, DYRK1A, EHMT1, FMR1, FOXG1, FOXP1, GABRB3, GAD1, GATAD2B, GRIA3, GRIK2, GRIN2A, GRIN2B, HDAC4, IL1RAPL1, IQSEC2, KATNAL2, KDM5C, KIRREL3, MBD5, MCPH1, MECP2, MED12, MED13L, MEF2C, MIB1, MTF1, MYH10, NLGN3, NLGN4X, NRXN1, NTNG1, OPHN1, PHF21A, PHF8, PPP2R5D, PQBP1, PTCHD1, PTEN, PTPN4, RAB39B, RAI1, RELN, RPS6KA3, SATB2, SCN2A, SETBP1, SHANK2, SHANK3, SLC6A1, SLC9A6, SYNGAP1, TANC2, TBR1, TCF4, TRIO, TUSC3, UBE3A, WAC

*NB: E' possible, su richiesta specifica, estrapolare dal pannello ed analizzare separatamente i soli geni ritenuti responsabili dello spettro fenotipico Sindrome di Angelman/Sindrome di Rett e Rett-like: UBE3A, SLC9A6, MECP2, CDKL5, FOXG1, MEF2C, TCF4, NTNG1, PTPN4

2. Genetic Background

The diagnosis of a MECP2 disorder is established by molecular genetic testing in a female proband with suggestive findings and a heterozygous MECP2 pathogenic variant. MeCP2 is expressed quite widely throughout the body, with notably high expression in postnatal neurons **[12, 18, 19].** However, the question remains why disruption of a ubiquitously expressed protein results in a predominantly neurological phenotype **[19]**. Most pathogenic mutations in MECP2 cause RTT in heterozygous females, whereas mutations leading to other phenotypic outcomes are also known **[29]**. Because most RTT cases are sporadic, it was difficult to map the disease locus by traditional linkage analysis; instead, using information from rare families, Xq28 region was identified and

subsequent screening of candidate genes in RTT patients revealed mutations in MECP2 **[3]**. Boys inheriting a mutant MECP2 allele are much more severely affected, presenting with infantile encephalopathy and usually not surviving infancy. Because most MECP2 mutations leading to RTT involve loss of function of the mutant allele, RTT can be modeled using gene knockout mice that recapitulate many of the key clinical signs that characterize RTT in humans **[10, 11]**.

MeCP2 is a member of a family of proteins that bind regions of DNA enriched with methylated CpG regions **[30]**. Containing a methyl-CpG binding domain and a transcriptional repression domain **[32, 33]**. MeCP2 was classically considered a methylation-dependent transcriptional repressor **[34]**. However, other studies suggest additional or alternative roles, including an enhancer of transcription **[6]** a global regulator of chromatin structure,38 or a global dampener of transcriptional noise **[7].**

MeCP2 is expressed in a range of tissues but is especially abundant in postmitotic neurons. Mice lacking MeCP2 in neurons show overt RTT-like symptoms, whereas mice in which the expression of MeCP2 is driven in neurons alone are reported to show a normal phenotype **[35]**. Although MeCP2 is present at low levels in astrocytes and MeCP2 deficiency in these cells may confer subtle noncell autonomous actions on neuronal phenotype **[37,38]** a body of evidence points to the overt RTT-like symptoms being due mainly to MeCP2 deficiency in the nervous system and neurons in particular.

3. Therapeutic Approaches

It appears that lack of functional MeCP2 results in a nervous system primed to malfunction at a critical point during postnatal brain development. However, function can be restored (including normal plasticity) to a large degree by the reintroduction of MeCP2.10 In the study by Guy et al **[10]** endogenous Mecp2 was silenced by insertion of a lox-stop cassette allowing the mice to develop symptoms (and plasticity deficits) before MeCP2 could be reintroduced into the brain by pharmacological reactivation of the gene. This reactivation resulted in a pronounced improvement in neurological signs and reduced mortality in the mice. Similar strategies to reintroduce or rebalance MeCP2 levels have been adopted by other groups using different genetic approaches and these studies have demonstrated improvements in motor function and a reversal of brain weight and neuronal morphology deficits **[36]**. Another genetic strategy has been to overexpress the brain-derived neurotrophic factor (BDNF, a potent modulator of synaptic plasticity/function that is dysregulated in MeCP2-mutant mice), which again reverses signs such as locomotor deficits. Although none of these studies represent a therapeutic strategy that can be applied to human patients, they nevertheless demonstrate the concept of phenotypic reversibility in mouse models of RTT and suggest that the Mecp2-mutant mice represent a viable platform for testing future pharmacological and genetic strategies that can be translated for clinical use.

The most obvious strategy in RTT is one of gene therapy. In contrast to the limited gene therapy literature, a significant number of studies have investigated pharmacological interventions in mouse models of RTT. Several modulators of synaptic function/plasticity have been tested, including the AMPA receptor modulator CX546, the insulin-like growth factor-1 tripeptide, the monoamine reuptake inhibitor desipramine, and the Alzheimer drug memantine. In addition to the pharma2cological strategies targeting neuronal mechanisms downstream of the MeCP2 deficiency, another approach is to target the MeCP2 mutation itself.

The studies focusing on AMPA receptor modulators (the ampakine CX546) are based on the fact that levels of BDNF are considered to be regulated by MeCP2 binding100 and that aberrant levels

of BDNF have concomitant effects on neurite outgrowth and synaptic maturation and maintenance. Mice treated with daily dosing of CX546 showed enhanced levels of BDNF and an improvement in the breathing phenotype (irregular breathing patterns), which is a prominent feature of RTT patients and seen in Mecp2-mutant mice **[33]**.

Another drug targeting glutamate receptors is the Alzheimer's drug memantine. This drug has recently been shown to be effective in other neurodevelopmental disorder models **[33]** and is well known to be effective in alleviating synaptic plasticity deficits. Weng et al **[34]** recently reported a synaptic plasticity saturation effect in the hippocampus of Mecp2-mutant mice and that impairment in both short- and long-term forms of synaptic plasticity can be partially reversed by memantine application in vitro when applied at clinically relevant concentrations. However, administration of memantine to Mecp2-mutant male mice was ineffective at preventing the onset of RTT-like signs and survival. Nevertheless, it remains to be tested whether memantine can afford cognitive benefits in females with a milder and stable RTT phenotype and mimic the human genotype.

In addition to BDNF (via ampakines), another growth factor that has received attention is IGF-1, which is a well-known regulator of synaptic maturation and plasticity. The activity of IGF-1 is regulated by a range of IGF-binding proteins. One of these, IGFBP3, has a binding site for the MeCP2 [104] and MeCP2-null mice and RTT patients express aberrantly high levels of this protein, which would be expected in turn to inhibit IGF-1 signaling **[35]**. An active tripeptide fragment of IGF-1 has been shown to enhance lifespan, improve locomotor function, and breathing pattern and heart rate abnormalities in MeCP2-null mice [70]. At the cellular level, reversed structural and cortical plasticity deficits were also observed following IGF-1 tripeptide treatment **[36]** and clinical trials using recombinant IGF-1 are now underway.

For some time, there has been an interest in monoamine systems with respect to RTT. There are consistent reports that levels of monoamine markers are reduced in the RTT brain and in MeCP2-null mice. To counter these deficits, drugs such as desipramine (an inhibitor of monoamine uptake) have been tested in MeCP2-null mice **[37, 38]**. Repeated administration of desipramine improves breathing and prolongs lifespan in RTT mice and at a cellular level, reverses the depletion in brain stem tyrosine hydroxylase **[39]**.

4. Neurophysiological Studies and Synaptic Plasticity

Most studies on RTT are done on mouse models, and can be summarized as follows:

1. Alteration in neuronal electrical properties within cortical areas and more pronounced changes in other regions such as the brain stem and locus ceruleus ;
2. Alteration in synaptic function include reduced synaptic plasticity;
3. Changes in basal inhibitory and excitatory synaptic transmission;
4. Changes in synaptic connectivity and neuronal structure whereas at the network level, there are changes in network excitability **[34;35;36]**.

Interestingly, synaptic plasticity (activity-dependent changes in the strength of synaptic communication) appears normal in young Mecp2-mutant mice **[10, 34, 35]** but shows impairment when tested in older mice on onset of overt RTT-like signs **[10, 35]**. Moreover, the degree of impairment appears to correlate with the severity of the RTT-like neurological phenotype (see **Figure 1**). The precise mechanisms underlying the involvement of MeCP2 in regulating

morphological and functional aspects of synaptic signaling remain to be identified. However, synaptic plasticity deficits are one of the most consistent findings and may provide important insights into RTT-like pathogenesis as well as serving as a target system for therapeutic interventions.

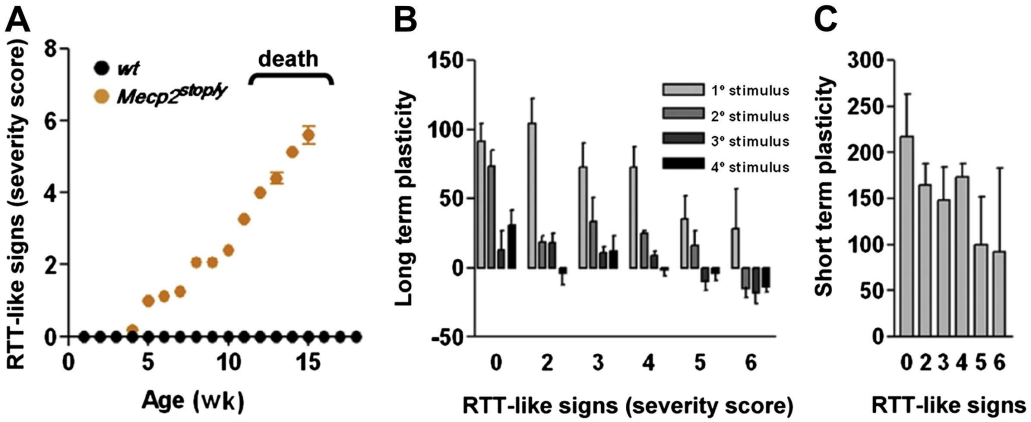

Figure 1. Symptomatic Mecp2-mutant mice show deficits in both long-term and short-term synaptic plasticity. (A) Time plot showing onset and progression of phenotypic (RTT-like) signs in male Mecp2-mutant mice (orange symbols). Wild-type mice (black symbols) invariably score 0. Note that Mecp2-mutant mice develop overt signs from around 5 weeks of age, with the severity score increasing over the subsequent 10–12 weeks. (B) Bar plot shows long-term plasticity following repeated (15 min interval) high-frequency stimulation. Note that in wild-type mice (Severity score = 0) the long-term plasticity level shows a robust and cumulative enhancement in response to second and subsequent high-frequency stimulation, whereas symptomatic Mecp2-mutant mice show reduced propensity to produce further long-term enhancement. (C) Bar plot showing levels of short-term plasticity (post-tetanic potentiation) are also progressively impaired as Mecp2-mutant mice develop RTT-like signs. From Weng et al103 with permission. RTT = Rett syndrome.

CLINICAL SETTING: NEUROPHYSIOLOGICAL SIGNATURES OF MOTOR IMPAIRMENT IN PATIENTS WITH RETT SYNDROME

1. Introduction

Motor impairment constitutes the core diagnostic features of RTT, such as partial or complete loss of acquired purposeful hand skills and spoken language, the development of gait abnormalities, stereotypic hand movements, and the progressive deterioration of motor abilities **[37]**. Although motor deficits are considered among the most debilitating symptoms of RTT individuals, little is known about the underlying pathophysiological mechanisms.

So far, the ability to model some aspects of the disease in the mouse, for instance by using knockout heterozygous female mice (ie, Mecp2+/−), provided the most significant clues for understanding the disease. At the cellular level, electrophysiological studies by means of whole cell patch clamp recordings showed alterations of synaptic excitability; the lack of MeCP2 induced a shift of the homeostatic balance between excitation and inhibition (E/I). Importantly, the direction of change of E/I in favor of excitation or inhibition depends on the specific brain circuit, even if recent evidence suggests that inhibition is reduced to a greater extent compared to excitation, thus enhancing the E/I ratio **[38]**. Interestingly, alterations in E/I balance have been shown to have consequences for cortical plasticity in neural circuits, and in this context, RTT has become one of the best disease models of abnormal synaptic plasticity **[37, 39, 40, 41]**. For instance, deficits of long-term potentiation (LTP) synaptic plasticity were observed at layer II/III synapses of motor and sensory cortex **[37]**; more recently, it has been shown that motor learning–dependent changes of parvalbumin expression and structural plasticity in the primary motor cortex (M1) were impaired in symptomatic Mecp2+/− female mice, and such defective cortical activity correlated with the severity of motor behavioral impairments **[42]**. The impairment of synaptic excitability and plasticity in M1 is particularly interesting given the anatomical evidence of a selective reduction of dendritic arborizations in pyramidal neurons of layers III and V of the frontal and motor cortices in human brain autopsies with RTT **[42, 43]**.

Although the mechanisms underlying E/I balance and cortical plasticity have been well studied in the mouse model of RTT, whether similar functional changes are present in humans with RTT is still unknown. To elucidate the physiological mechanisms associated with motor impairment in humans with RTT, we tested the function of excitatory and inhibitory circuits and the level of LTP-like activity in M1 using noninvasive brain stimulation techniques. Transcranial magnetic stimulation (TMS) was used to probe cortical excitability and plasticity in people with RTT. TMS activates human motor cortex transcranially; specifically, according to the microcircuit model **[44,45]** TMS induces strong depolarization of layer II/III pyramidal and inhibitory cells that in turns leads to highly synchronized recruitment of clusters of excitatory neurons, including pyramidal neurons of layer V, that represent the major output of M1 **[44, 45]**. Protocols of paired pulse TMS may provide insights into the function of cortical inhibitory and excitatory interneurons depending on the interval between the conditioning and test stimuli **[46,47]** and repetitive TMS (rTMS) evaluates LTP-like activity of central motor circuits and thus can reveal abnormalities in brain plasticity **[46, 47]**. Herein, we used patterned rTMS, namely intermittent theta burst stimulation (iTBS), to investigate LTP within M1 (**Table 1**) **[46]**.

We hypothesized that RTT patients would exhibit a lack of cortical plasticity together with a shift toward excitation of the E/I balance, likely due to a reduction of inhibitory mechanisms, and these alterations would scale with motor deficit. As an ancillary investigation, we assessed the serum level of insulin like growth factor 1 (IGF-1), which is demonstrated to be reduced in a mice model

of RTT **[50]**. In mice, the administration of IGF-1 partly reversed clinical phenotype, **[50, 51]** restoring cortical plasticity **[50,51,52]** and normalizing the E/I balance. In humans, the first clinical studies on the therapeutic use of IGF-1 reported promising effects **[48, 53]**; however, recent placebo controlled trials provided conflicting results **[54, 55, 56].**

2. Patients and Methods

Patients and Clinical Evaluation

The study complied with the Helsinki declaration on human experimentation and was approved by the Ethical Committee of the University of Naples Federico II (n. 100/17). Parents or legal guardians of the participants gave informed consent. Participants were seen at the Child Neuropsychiatric Department or Epilepsy Center of the University of Naples Federico II between 2017 and 2018.

For RTT patients, a history and structured examination was performed for each girl by experienced examiners (P.B, C.B.) to confirm the diagnosis using consensus criteria **[14]**. Individuals were included if they met the consensus criteria for typical RTT,24 carried MECP2 mutations, and had a complete clinical assessment by means of dedicated clinical scales: the clinical severity score (CSS) **[57]** and the Rett Syndrome Gross Motor Scale (RSGMS) **[58]**.

Because the main aim of the study was to evaluate the impact of motor disability on neurophysiological measures in M1, we decided to use only the motor-skill categories of the CSS, namely the hand use, motor/independent sitting, and ambulation items. Each item score ranges from 0 to 4 or 0 to 5, with 0 representing the less severe and 4 or 5 representing the most severe finding **[57]**. For example, in the ambulation category, a score of 2 or less indicates the ability to walk alone, whereas a score of 3 or higher indicates that the individual cannot walk unaided or is completely unable to walk. Similar divisions can be made for the hand use and motor/independent sitting category. In addition, to further evaluate motor skills, we applied the RSGMS that measures gross motor abilities by considering 15 gross motor skills scored on a 0 to 3 scale, ranging from maximal assistance/unable (score = 0) to no assistance (score = 3) **[58]**. By using these scores, we asked whether the magnitude of alteration in plasticity and E/I balance in M1 would be correlated with motor performance. Although CSS is considered less sensitive and reliable than RSGMS in evaluating longitudinal gross motor function, we adopted both scales to have a cross-validation of our data, providing a conceptual within-study replication that would strengthen the reliability of our results. Lastly, control data were gathered from 9 subjects with non-RTT epilepsy taking antiepileptic drugs (AED) and 11 healthy participants.

Table 1

TMS-EMG Measures	Protocol	Putative Mechanisms	Effects of CNS Active Drugs on TMS–EMG Measures
Motor thresholds: RMT, AMT	Single pulse: the minimum TMS intensity that is necessary to elicit a liminal MEP in the target muscle, either at rest (RMT) or during slight voluntary contraction (AMT)	Cortical motor neuron voltage-gated sodium channel–mediated membrane excitability	Increased by voltage-gated sodium channel blockers (eg, carbamazepine, lamotrigine, phenytoin); decreased by NMDA-type and AMPA-type glutamate receptor antagonists (eg,

			ketamine)
Short-interval intracortical inhibition	Paired pulse: subthreshold conditioning stimulus and suprathreshold test stimulus applied at short interstimulus intervals of 1–5 milliseconds	GABAA-mediated cortical inhibition	Increased by GABAA-positive allosteric modulators (eg, lorazepam)
Intracortical facilitation	Paired pulse: subthreshold conditioning stimulus and suprathreshold test stimulus applied at interstimulus intervals of 7–20 milliseconds	GABAA-mediated cortical inhibition; glutamate mediated cortical excitation	Decreased by GABAA-positive allosteric modulators (eg, diazepam, lorazepam) and NMDA-type and AMPA-type glutamate receptor antagonists (eg, memantine)
Long-interval intracortical inhibition	Paired pulse: 2 suprathreshold stimuli applied at long interstimulus intervals of 50–300 milliseconds	GABAB-mediated cortical inhibition	Increased by GABAB agonists (eg, baclofen, tiagabine, vigabatrin)
Intermittent theta burst stimulation	Patterned repetitive stimulation: 600 subthreshold pulses (10 bursts of triplets at 50Hz, in short trains of 2 seconds, with an 8-second pause between consecutive trains)	Glutamate-mediated LTP-like plasticity	Decreased by NMDA-type glutamate receptor antagonists (eg, memantine), L-type voltage-gated ion channel blockers (eg, nimodipine), and type 2 dopamine receptor antagonist (eg, sulpiride)

AMPA = α-amino-3-hydroxy-5-methyl-4-isoxazolepropionic acid; AMT = active motor threshold; CNS = central nervous system; EMG = electromyography; GABA = γ-aminobutyric acid; LTP = long-term potentiation; MEP = motor evoked potential; NMDA = N-methyl-D-aspartate; RMT = resting motor threshold; TMS = transcranial magnetic stimulation.

Electrophysiology

Electromyographic Recording and Focal TMS. Participants were seated comfortably in a chair reposing both hands suitably on a cushion or their lap to ensure complete relaxation. Motor evoked potentials (MEPs) were recorded by electromyography (EMG) from the right first dorsal interosseous (FDI) muscle using Ag–AgCl surface electrodes (Ambu, Ballerup, Denmark) mounted using the belly-tendon technique. The signals from the EMG electrodes were amplified, bandpass filtered (20Hz–3kHz), digitized at a frequency of 5kHz, and stored in a laboratory computer for later offline analysis by Signal software and CED 1401 hardware (Cambridge Electronic Design, Cambridge, United Kingdom). The level of baseline EMG activity was controlled by visual feedback through an oscilloscope screen and by auditory feedback through a loudspeaker. We rejected trials with involuntary EMG activity from FDI muscle greater than 50μV in a time window of 500 milliseconds preceding MEPs.

Focal TMS was performed using a figure-of-8–shaped magnetic coil (outer diameter of each wing 70mm) that was held tangentially to the skull with the handle pointing backward and laterally at an

angle of 45° to the sagittal plane (direction of current induced in the brain: posterior to anterior). Experiments were performed by connecting the coil to a high-power magnetic stimulator with a biphasic current waveform (MagPro X100; Medtronic, Skovlunde, Denmark). The "hot spot" was defined as the optimal scalp position for eliciting MEPs of maximal amplitude in the contralateral FDI. To ensure stability of the stimulation position over the course of the experiment, the hotspot was marked directly on the scalp with a soft-tip pen. Measures of Motor Thresholds and Intracortical Inhibitory/Excitatory Balance. Resting motor threshold (RMT) was determined as the minimum stimulator intensity needed to produce a response of at least 50μV in the relaxed FDI in at least 5 of 10 consecutive trials. Active motor threshold (AMT) was calculated during a mild tonic contraction (approximately 20% of maximal contraction) as the lowest intensity evoking 5 MEPs of at least 200μV in 10 consecutive trials **[59]**. In the case of RTT patients, muscle contraction was obtained by placing a weight in the outstretched, supinated hand, with the arm adducted at the shoulder and flexed at the elbow to about 90°; for less cooperative patients, muscle contraction was elicited using the traction reflex. In addition, to check if muscle contraction gave reliable AMT results in RTT patients, we normalized the AMT value with respect to the RMT and compared this ratio among the 3 groups. To assess inhibitory/excitatory balance in M1, we applied 2 paired-pulse TMS protocols: short-interval intracortical inhibition (SICI) and intracortical facilitation (ICF). SICI is supposed to be mediated by GABAA-ergic intracortical circuits, and ICF is mediated by glutamatergic intracortical circuits, possibly alongside a reduction in GABAergic inhibition (**see Table**) **[46]**. SICI and ICF were determined by setting the conditioning stimulus (CS) intensity to 95% AMT and delivering the CS before the test stimulus (TS). For both paradigms, the unconditioned MEP (TS) was adjusted to evoke an MEP of ~0.5mV amplitude in the right FDI muscle. A previous study showed that SICI and ICF can be observed with TS intensity of 0.5mV **[60]**. SICI was recorded at interstimulus intervals (ISIs) of 2 and 3 milliseconds, **[61]** and intracortical ICF was determined at ISIs of 10 and 15 milliseconds; then they were expressed as the mean peak-to-peak amplitude normalized with respect to the TS **[62]**. Subsequently, the average of normalized SICI and ICF, over the different ISIs, was measured for each patient. To express the balance between cortical inhibitory and facilitatory interneuronal function, an excitation index was developed and expressed in the following formula:

Excitation index = ICF/ ICF −SICI

Lastly, we applied the long-interval intracortical inhibition (LICI) that is supposed to be mediated by GABAB-ergic intracortical circuits within M1 (**see Table**) **[46, 63]**. LICI was investigated by implementing 2 suprathreshold stimuli, with the CS adjusted at 120% of the RMT, with ISIs of 100 and 150 milliseconds (**Fig 1**) **[64]**. For all paired-pulse paradigms, 15 trials were recorded for each condition and randomly intermixed with 15 trials of TS alone (0.2Hz +/- 10%). Complete voluntary muscle relaxation was monitored audio visually by high-gain EMG (50μV/division). Trials contaminated with voluntary activity were discarded from the analysis **[65]**.

Assessment of Cortical Plasticity after iTBS. We applied iTBS using the well-known paradigm introduced by Huang et al.16 It consisted of bursts of 3 pulses at high frequency, 50Hz, repeated at intervals of 200 milliseconds, delivered in short trains lasting 2 seconds, with an 8-second pause between consecutive trains, for a total of 600 pulses (**see Fig 1**). The stimulation intensity for iTBS was set at 80% AMT. To assess corticospinal excitability before iTBS, single MEPs were recorded using a stimulus intensity adjusted to produce MEP amplitude of approximately 0.5mV in the relaxed FDI muscle. For each subject, 20 MEPs were recorded, and the peak-to-peak amplitudes were measured to calculate the mean amplitude.

After the interventions, corticospinal excitability changes were monitored by collecting 12 MEP responses (0.2Hz +/- 10%) every 2 minutes following the intervention for up to 30 minutes (15 blocks, starting with 2 minutes of rest, then 1 minute measurement, 1minute rest, and so on (**see Fig 1**) **[66, 67]**. We decided to adopt a high temporal resolution of corticospinal excitability assessment after iTBS for a better estimation of the different patterns of motor cortex plasticity across the groups over time **[66, 67]**. The average duration of the whole experiment in a single subject was 55 minutes: 20 minutes for the evaluation of motor thresholds and inhibitory/facilitatory circuits and 35 minutes for the assessment of motor cortex plasticity.

IGF-1 Measurement

Serum IGF-1 concentration was determined by a solid-phase, enzyme-labelled chemiluminescent immunometric assay (IMMULITE 2000; Siemens Healthcare Diagnostics, Tarrytown, NY). IGF-1 concentration was expressed as standard deviation score (SDS) according to the normative data provided by the manufacturer. SDS ≤ -2.5 was considered abnormal.

Statistical Analysis

Data were analyzed using IBM SPSS Statistics v.22.0 for Windows (IBM, Armonk, NY). Normal distribution was verified by means of Kolmogorov and Smirnov test. One-way analysis of variance (ANOVA) was applied to compare age, motor thresholds, and excitation index in the 3 groups: RTT patients, epilepsy controls, and healthy subjects. The same test was also applied to ensure that amplitude of TS for different paired-pulse paradigms (SICI–ICF and LICI) and MEP amplitudes before iTBS did not differ across groups. Then the effect of SICI–ICF and LICI (normalized values) were compared with a 2-way mixed-model ANOVA, with "ISI" as within-subjects factor and "group" as between-subjects factor. When dealing with iTBS, a 2-way mixed-model ANOVA was performed on MEP amplitude expressed as percentage of change in comparison to baseline, with "time" as within subjects factor and "group" (RTT, epilepsy controls, and healthy controls) as the between-subjects factor. If a significant main effect was obtained, group differences were examined with post hoc tests (Bonferroni correction for multiple comparisons). The Greenhouse–Geisser method was used to correct for non sphericity whenever necessary.

Correlation between IGF-1 (SDS), clinical scores (disease duration, CSS motor score, RSGMS), and the main neurophysiological parameters (excitation index, mean amplitude change of MEP after iTBS, and the mean inhibition at LICI) were evaluated using Pearson correlation coefficient. Alpha inflation due to multiple comparisons was controlled according to Bonferroni approach when appropriate. Effects were considered significant if $p < 0.05$. All data are presented as mean +/- standard error of the mean (SEM) if not stated otherwise.

Figure 1

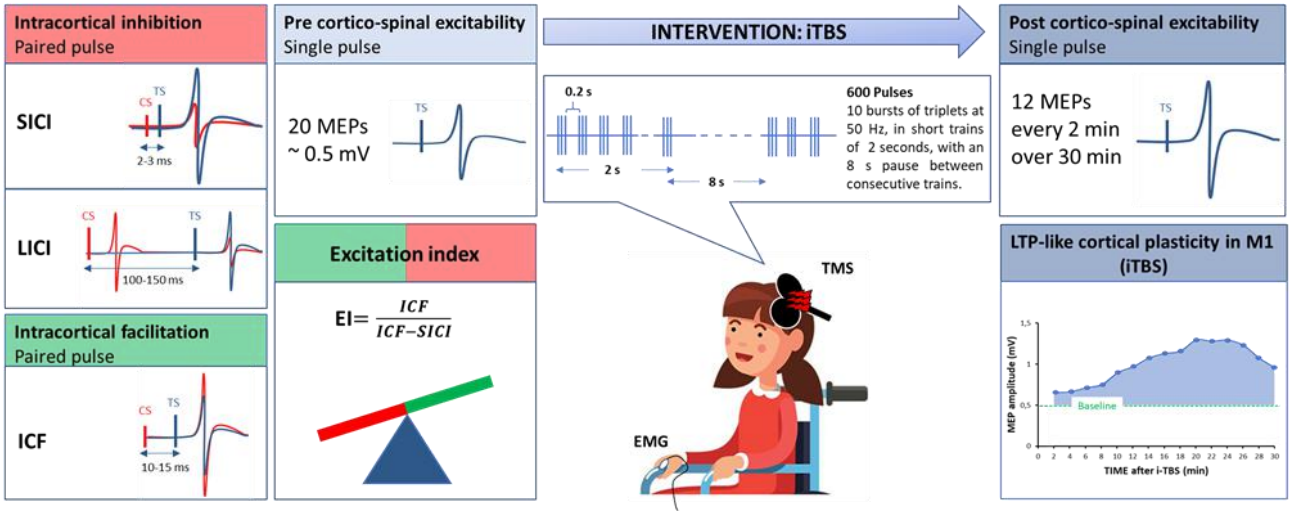

FIGURE 1: Schematic overview of experiment. Before the intervention, participants underwent motor threshold assessment, namely resting and active motor thresholds (not shown), intracortical inhibitory (short-interval intracortical inhibition [SICI], long-interval intracortical inhibition [LICI]), and facilitatory circuit (intracortical facilitation [ICF]) evaluation by means of paired-pulse transcranial magnetic stimulation (TMS) protocols. In addition, to evaluate the balance between facilitation and inhibition within the motor cortex, we computed the excitation index (EI), expressed here as the ratio between ICF and SICI. Lastly, just before the application of the intermittent theta burst (iTBS), corticospinal excitability was evaluated by recording 20 motor evoked potentials (MEPs) at around 0.5mV of amplitude. Following the intervention (horizontal arrow) subjects paused for 2 minutes, and post-iTBS corticospinal excitability was established by obtaining MEP responses (15 blocks consisting of 12 MEP responses each, with each followed by 1 minute of rest) up to 30 minutes after intervention. CS = conditioning stimulus; EMG = electromyography; LTP = long-term potentiation; M1 = primary motor cortex; TS = test stimulus.

Figure 2

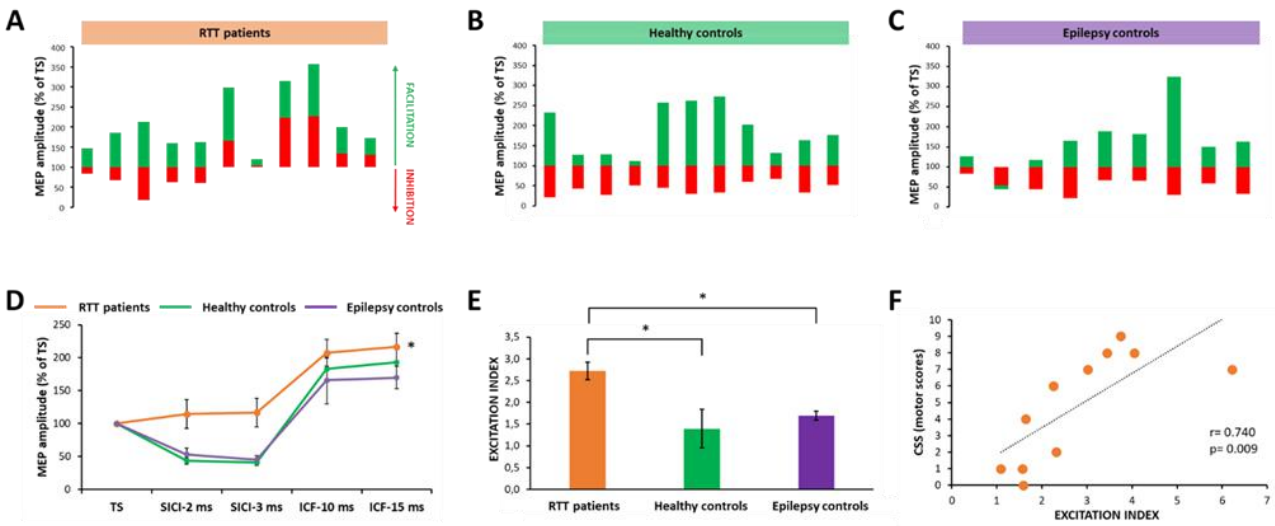

Balance between SICI and ICF circuits in patients with RTT, epilepsy and healthy controls Average of short-interval intracortical inhibition (SICI, red bars) and intracortical facilitation (ICF, green bars) expressed as a percentage of test stimulus (TS) in individual (A) Rett syndrome (RTT) patients (B) healthy controls and (C) epilepsy controls. Group average data normalized respect to TS for each Interstimulus interval of SICI and ICF (D) showing the lack of inhibition in RTT patients (orange line). The Excitation index, a biomarker reflecting the contribution of inhibitory and facilitatory circuit activity, is significantly increased in RTT patients compared to the other two groups, suggesting a shift toward cortical excitation (E). A non-significant trend was evident for the correlation between the Excitation index and motor score indexed by the clinical severity score (CSS) (F). *= statistically significant. TS= Test stimulus.

Figure 3

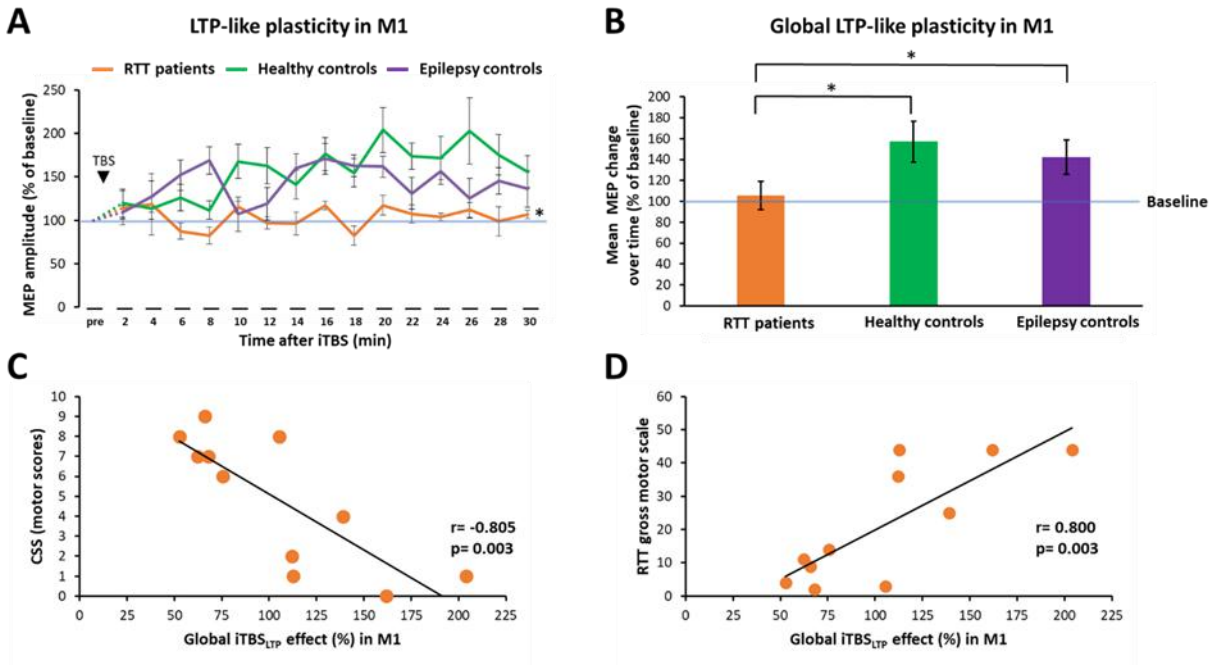

LTP-like plasticity in the primary motor cortex (M1) Time course of MEP amplitude change over time: (A) each line represents the group average in MEP responses normalized to pre-iTBS. Note a significant loss of LTP-like plasticity in M1 only in Rett patients. Arrowheads represent time of iTBS intervention. Small gaps in the x-axis indicate interruptions for each 1 min break. (B) Synopsis of the overall MEP change (normalized to baseline) after iTBS in each group, confirming the lack of LTP-like plasticity in RTT group (orange bar) respect to healthy controls (green bar) and epilepsy patients (violet bar). The gain of M1 excitability after iTBS scaled with motor performance, indexed by motor items of the Clinical Severity Score (CSS) and the RTT gross motor scale (C, D). Significant correlations are indicated by a bold continuous regression line (p< 0,004 after Bonferroni correction for multiple comparisons). TS= Test Stimulus. *= statistically significant.

Figure 4

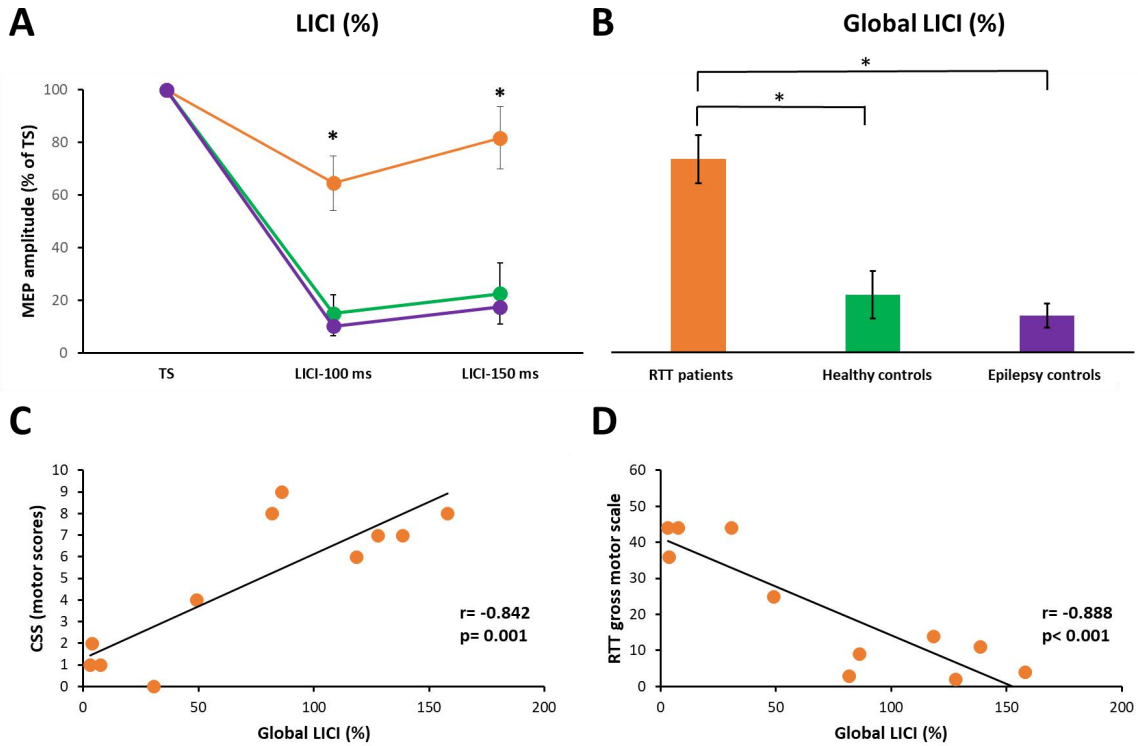

Clinical correlates of neurophysiological abnormalities in patients with Rett syndrome. Group data for LICI (Long Interval Cortical Inhibition) confirms the lack of inhibition in RTT patients for each ISI (Interstimulus interval) (A) and for the Global LICI, obtained averaging ISIs at 100 and 150 ms. Clinical motor scores (Clinical severity score, CSS, and Rett Syndrome gross motor scale) correlates with the amount of inhibition in the primary motor cortex (M1), indexed by the global LICI (C-D). The higher was the amount of inhibition the better was the motor phenotype. Significant correlations are indicated by a bold continuous regression line ($p < 0.004$ after Bonferroni correction for multiple comparisons). TS= Test Stimulus. *= statistically significant.

3. Results

Participants

Fourteen young adults with RTT were recruited (mean age = 22.64 +/- 2.12 years); 11 had fullTMS testing, and 3 participants were excluded because of high motor thresholds (Supplementary Tables 1 and 2). Nine people with epilepsy taking AEDs (E1–E9; mean age = 25.11 +/- 2.56 years) and 11 healthy participants (mean age = 22.64 +/- 1.75 years) were recruited as control groups. All healthy participants and epilepsy controls were right-handed females. Supplementary Table 1 shows demographic information, genetic diagnosis (for those with RTT), epilepsy diagnosis (for epilepsy controls), and medication at time of testing. There was no significant difference in age among the 3 groups (1-way ANOVA $F_{2, 33} = 0.386$, $p = 0.683$).

Table 1

Participant	Age (y)	MECP2 mutation or epilepsy diagnosis	Medication at time of testing, mg/d	Serum IGF-1 level, SDS	CSS (Motor/ Indipendent sitting)	CSS (Ambulation)	CSS (hand use)	CSS (sum motor score	RTT Gross Motor scale

								)	
RTT	31	p.T158M	PHB 100	0.05	0	0	2	2	36
RTT	16	p.R306C	VPA 800	-2.1	0	0	1	1	44
RTT	23	p.K305N	NT	2.06	0	0	1	1	44
RTT	13	p.Lys144ArgfsX2	NT	-0.23	0	2	2	4	25
RTT	16	p.[(G354Rfs*44)]	VPA 700	-1.46	0	0	0	0	44
RTT*	16	p.Leu150Ser	LEV 1200, VPA 650, TPM 175	-0.57	0	1	1	2	34
RTT	17	c.1072_1186del	CBZ 1200, TPM 225	0.2	1	3	2	6	14
RTT	29	p.R255X	LTG 250	-0.85	1	3	3	7	11
RTT	18	p.N126Y	LEV 1600, CLB 10	1.62	0	5	3	8	3
RTT	42	p.R270X	CBZ 600	1.78	2	4	3	9	9
RTT	27	p.R168X	LCM 100, CBZ 500, CLN 14	-0.53	1	4	2	7	2
RTT*	20	p.R270X	CBZ 400, PHB 50	0.54	3	5	3	11	2
RTT	29	p.Pro385fs	LTG 250, CBZ 600	0.85	2	3	3	8	4
RTT*	18	p.R255X	LTG 125, VPA 500	0.48	1	5	2	8	4
E1	20	JME	VPA 500, LEV 100						

E2	22	TLE (unknown cause)	CBZ 500, LTG 200
E3	42	JME	VPA 750, LEV 3000
E4	32	JME	VPA 450, LEV 2000, LTG 200
E5	20	JME	VPA 750, LEV 1250, LTG 200
E6	28	GGE	VPA 500, FBM 2450
E7	20	FLE (unknown cause)	LCM 200, CBZ 500
E8	23	JME	LTG 350, CLB 10
E9	19	GGE	LEV 3000, BRIV 100, CBZ 1200

*Table 1: Age, mutation (patients with Rett syndrome (RTT) only), epilepsy diagnosis (epilepsy controls (E) only), clinical motor scores (patients with RTT only) medication at time of testing for all participants. Abbreviations: BRIV = brivaracetam; CBZ = carbamazepine; CLB = clobazam; CLN = clonazepam; CSS = clinical severity score; FBM = felbamate; FLE = frontal lobe epilepsy; GGE = genetic generalized epilepsy; JME= juvenile myoclonic epilepsy; LCM = lacosamide; LEV = levetiracetam; LTG = lamotrigine; NT= no therapy; OXC = oxcarbazepine; PHB = phenobarbital; TPM = topiramate; VPA = valproate; RTT= Rett syndrome; SDS= standard deviation score. *****= discarded from TMS study because of high motor thresholds.*

Table 2

Participant	RMT (%)	AMT (%)	SICI (%)	ICF (%)	LICI (%)	$iTBS_{LTP}$ (%)
RTT	49	40	83.96	147.57	3.66	112.01
RTT	70	64	67.18	185.67	7.46	112.86
RTT	38	33	17.87	213.33	3.01	203.92
RTT	48	40	62.42	160.32	49.03	138.97
RTT	58	48	60.37	162.48	30.62	142.72
RTT*	-	-	-	-	-	-
RTT	75	58	166.05	298.02	118.31	75.67
RTT	63	43	100.38	119.62	138.49	62.36
RTT	50	45	223.12	314.26	81.74	105.39
RTT	80	69	226.85	356.48	86.16	65.99
RTT	65	51	133.68	199.83	127.79	88.11

RTT*	-	-	-	-	-	-
RTT	65	52	130.19	172.87	158	52.74
RTT*	-	-	-	-	-	-
E1	63	44	46.71	126.44	11.19	155.40
E2	59	47	54.02	98.10	2.75	193.95
E3	60	45	44.04	116.75	11.01	172.47
E4	58	53	21.67	165	32.74	127.71
E5	72	53	66.86	188.31	3.69	160.61
E6	65	60	65.82	180.50	36.94	182.81
E7	52	47	30.95	324.60	6.08	106.11
E8	62	53	58.00	149.94	17.35	124.48
E9	57	50	32.86	163.45	2.62	136.98

Table 2

Transcranial magnetic stimulation findings.

*Abbreviations: E= epilepsy control; RTT= Rett syndrome; RMT= resting motor threshold; AMT= active motor threshold; SICI= short-interval intracortical inhibition; ICF= intracortical facilitation; LICI= long-interval intracortical inhibition; iTBSLTP = long term potentiation like plasticity induced by intermittent theta burst stimulation; *****= discarded from TMS study because of high motor thresholds. Motor thresholds are expressed as % of the maximum stimulator output; SICI is expressed as the mean (%) of inhibition obtained averaging interstimulus interval at 2 and 3 ms; ICF is expressed as the mean (%) of facilitation obtained averaging interstimulus interval at 10 and 15 ms; LICI is expressed as the mean (%) of inhibition obtained averaging interstimulus interval at 100 and 150 ms; iTBSLTP is expressed as the mean (%) of the MEP amplitude change over time.*

Motor Thresholds

One-way ANOVA comparingmotor thresholds in all 3 groups showed significant differences for both RMT ($F_{2, 30} = 21.734$, $p < 0.001$) and AMT ($F_{2, 30} = 19.925$, $p < 0.001$); post hoc analysis confirmed a significant difference only between patients (RTT and epilepsy controls) and healthy subjects (all $p < 0.001$), with RMT and AMT higher in patients (RTT group: RMT = 60.09 +/- 3.86, AMT = 49.36 +/- 3.29; epilepsy controls: RMT = 60.89 +/- 1.87,AMT = 50.22 +/- 1.69) with respect to healthy participants (RMT = 37 +/- 2.39; AMT = 30.36 +/- 2.09). Interestingly, motor thresholds of the 2 RTT patients not taking AEDs were within the normal limits (RMT = 38 and 48, upper limit <50; AMT = 33 and 38, upper limit <42; see Supplementary Table 2). Overall these results confirm the well-known effect of AEDs on increasing motor thresholds.13,14,36 In addition, muscle contraction gave reliable AMT results in RTT patients; paired t test showed that AMT values were consistently lower than RMT in each participant (t test: $p < 0.001$), and AMT values normalized with respect to RMT were almost identical among the 3 groups (RTT: 0.82 +/- 0.02, epilepsy controls: 0.82 +/- 0.02, healthy participants: 0.83 +/- 0.03), as confirmed by 1-way ANOVA ($F_{2, 30} = 0.026$, $p = 0.975$).

Intracortical Inhibitory and Facilitatory Circuits and the Excitation Index

For SICI–ICF, mixed-model ANOVA yielded a group effect ($F_{2, 28} = 4.241$, $p = 0.025$), and post hoc comparisons showed that RTT patients exhibited an overall altered modulation for intracortical and facilitatory circuits tested by SICI–ICF with respect to the other 2 groups ($p < 0.022$). As

expected, we also showed a main ISI effect ($F_{2.15, 60.27} = 56.657$, $p < 0.001$; Greenhouse–Geisser correction: $\varepsilon = 0.718$) because MEPs were inhibited at short ISIs (ie, 2 and 3 milliseconds), whereas for longer ISI (ie, 10 and 15 milliseconds) the inhibition was replaced by facilitation (Fig 2). Instead, the interaction ISI × group did not reach any statistical significance ($F_{4.31, 60.27} = 0.903$, $p = 0.474$; Greenhouse-Geisser correction: $\varepsilon = 0.718$). To determine the balance between inhibitory and facilitatory circuits in M1, an excitation index was developed. The excitation index was higher in RTT patients (2.72 +/- 0.44, ANOVA: $F_{2, 30} = 9.979$, $p = 0.003$) compared to epilepsy controls (1.69 +/- 0.08, $p = 0.007$) and healthy participants (1.39 +/- 0.10, $p = 0.002$; see Fig 2). Taken together, these findings suggest a dynamic shift in the balance between facilitatory and inhibitory circuits in RTT, with a preponderance to net motor cortex hyperexcitability, likely due to reduced GABAergic activity. Impairment of GABAergic activity was also confirmed by LICI, showing a main effect of group ($F_{2, 28} = 8.265$, $p = 0.002$). Post hoc testing revealed that only RTT group exhibited an overall reduction of the inhibition's magnitude probed by LICI (all $p < 0.002$; Fig 3). Mixed-model ANOVA also showed a main effect of ISI ($F_{1, 28} = 7.851$, $p = 0.009$) providing stronger inhibition at 100 milliseconds than at 150 milliseconds for all participants (31.49 +/- 7.9 vs 43.79 +/- 8.87). On the contrary, the interaction ISI × group did not reach any statistical significance ($F_{2, 28} = 0.449$, $p = 0.643$).

Cortical Plasticity Induced by iTBS Baseline mean MEP values (pre-iTBS) did not differ across groups (1-way ANOVA: $F_{2, 30} = 1.081$, $p = 0.353$). Regarding corticospinal excitability after iTBS, the mixed-model ANOVA showed a significant group effect ($F_{2, 28} = 5.687$, $p = 0.008$), suggesting a different modulation of excitability enhancing effect of iTBS among groups. Specifically, post hoc comparisons revealed that RTT patients did not exhibit the physiological enhancement of corticospinal excitability following iTBS (all $p < 0.014$; Fig 4 and Supplementary Table 2). ANOVA also revealed a significant effect of time ($F_{14, 392} = 2.765$, $p = 0.001$), indicating a different modulation of MEP amplitudes over time. Lastly, the interaction time × group did not show any statistical significance ($F_{28, 392} = 1.485$, $p = 0.056$).

Clinical Correlates of Neurophysiological Abnormalities in RTT

To evaluate the clinical significance of the described neurophysiological abnormalities, we performed correlation analyses between the motor scores and the main neurophysiological parameters. Significant correlations ($p < 0.004$ after Bonferroni correction for multiple comparisons) were obtained contrasting CSS motor scores with the global mean inhibition indexed by LICI ($r = 0.842$, $p = 0.001$) and with the overall gain of corticospinal excitability after iTBS ($r = -0.805$, $p = 0.003$). We observed the same significant results for the RSGMS (LICI: $r = -0.888$, $p < 0.001$; iTBS: $r = 0.800$, $p = 0.003$). On the contrary, a nonsignificant relationship was evident for the excitation index (CSS–motor: $r = 0.740$, $p = 0.009$; RSGMS: $r = -0.708$, $p = 0.015$) and for the correlation between disease duration and the mean corticospinal excitably gain after iTBS ($r = -0.677$, $p = 0.022$). The remaining correlations showed a nonsignificant trend, either contrasting neurophysiological measures with disease duration (all $p > 0.052$) or age (all $p > 0.084$). These results suggest that motor disabilities in RTT patients impact negatively on the motor cortex plasticity and the efficacy of inhibitory circuits within M1. Instead, the lack of significant results with disease duration and age might be due to the small sample size or age range. IGF-1 Levels IGF-1 levels, expressed as SDS, were within the age range for all RTT patients (range = −2.1 to 2.06). No significant correlation was found when contrasting IGF-1 levels with neurophysiological parameters (excitation index: $r = 0.68$, $p = 0.844$; iTBS LTP: $r = 0.77$, $p = 0.821$; mean LICI: $r = 0.085$, $p = 0.805$) and clinical scores (CSS: $r = 0.473$, $p = 0.088$; RSGMS: $r = -388$, $p = 0.170$).

4. Discussion

To the best of our knowledge, this is the first study showing abnormalities of the E/I balance and LTP-like plasticity in M1 of humans with RTT. These alterations were associated with a greater degree of functional motor disabilities, suggesting a pathophysiologic role of these functional changes.

E/I Balance Shifts toward Excitation in M1 of RTT

The dysfunction of excitatory and inhibitory motor circuits contributes to the development of cortical hyperexcitability in RTT. Specifically, there was a reduction of SICI along with an increase in ICF, suggesting a disinhibition of intracortical circuits in RTT group. The excitation index, which captures the balance between short-latency interneuronal inhibition and long-latency facilitation, was significantly shifted toward an excitatory drive in patients with RTT.

The precise mechanisms underlying the development of hyperexcitability in M1 remain unresolved. Interestingly, although different synapses in distinct parts of the brain are differentially modulated upon loss of MECP2, recent preclinical evidence has suggested a common direction of change in E/I balance in favor of excitation **[32, 33]**. Intracellular recordings in cortical neuron reveal that inhibition and excitation are both reduced in Mecp2 knockout mice, but inhibition is reduced to a greater degree, thus enhancing the E/I ratio **[39]**. In addition, in vivo functional measurements of inhibitory conductance in adult Mecp2 knockout mice, along with reduced responses of parvalbumin-expressing (PV+) interneurons, consistently revealed reduced inhibition in cortical circuits.5 PV interneurons are powerful regulators of pyramidal neuron activity and appear to be critical regulators of the E/I balance in human neocortex.

Importantly, our neurophysiological results seem to confirm that the increase of E/I ratio might be due to the reduced efficiency of inhibitory circuits within M1. ICF has been demonstrated to be decreased by GABAergic agonists that would conversely increase SICI **[46]**. Consequently, the decrease of SICI together with the increase in ICF could be partly consistent with the disinhibition of layer V pyramidal neurons, resulting in an enhanced corticospinal output.

Deficits of intracortical inhibitory circuits also have been confirmed by the reduction of LICI, which, according to pharmaco-TMS studies, is supposed to be mediated by GABAB network **[46]**. We found that the amount of LICI scaled with clinical motor scores; namely, the worse the motor performance, indexed by the CSS motor scale and RSGMS, the lower the magnitude of inhibition. Dysregulation of PV inhibitory interneuron expression, observed in M1 of Mecp2 knockout mice, also correlated with the severity of motor behavioral impairments **[41]**.

Reductions of central motor conduction time and of cortical silent period assessed by TMS have been previously reported in patients with RTT and mainly explained by degeneration of inhibitory circuits **[70, 72]**. Specifically, the authors suggested a possible “upstream” disorder, involving cortical inhibitory interneurons and consequently influencing the outflow of the pyramidal cells in M1.38 Therefore, we reason that the shortening of the central motor conduction time could be in line with our findings of altered intracortical inhibitory circuits, as suggested by the reduced magnitude of LICI and the increased excitation index.

Lastly, we also observed higher motor thresholds in our patient groups, that is, RTT and epilepsy controls. It is well known that anticonvulsant medication might elevate motor thresholds **[46, 47, 50]**. This may account for the higher thresholds in patients relative to healthy subjects, but it seems unlikely that it explains the difference in E/I balance and motor cortex plasticity seen between the 2

similarly treated patient groups. This observation also should be considered when assessing previous results of motor threshold level in RTT patients **[70, 72]**. Specifically, the study by Krajnc and Zidar **[72]** showed elevated motor thresholds even in those RTT patients not taking AEDs, whereas in our study motor thresholds were normal. Differences in the results of their study versus ours might be due to methodological dissimilarities, such as the use of a different target muscle (abductor digiti minimi vs FDI), TMS pulse waveform (monophasic vs biphasic stimulation), and RMT assessment method (100μV vs 50μV). In addition, the study of Eyre and colleagues [70] showed opposite findings—lower motor thresholds in RTT patients compared to healthy controls–suggesting a possible impairment of inhibitory controls on pyramidal neurons in M1. In this multicenter study, which includes a larger sample of RTT patients not taking AED, we could reach a definite conclusion.

Loss of Motor Cortex Plasticity Is Associated with Motor Deficits in RTT

The current study demonstrates robust evidence for deficit of LTP-like cortical plasticity in the M1 of RTT patients. An important observation is that motor cortex plasticity impairment parallels motor deficit being more seriously affected in patients with severe motor symptoms. Interestingly, our results are consistent with those of previous studies conducted in mice, where the deficit in cortical synaptic plasticity appeared with the onset of overt RTT like symptoms. In these studies, the investigation of LTP alterations has been consistently described in the hippocampus **[73, 76]** and less frequently in M1 **[40]**. Synaptic plasticity deficit in the hippocampus can be observed in very mildly symptomatic male mice, and with symptom progression these subtle abnormalities in synaptic plasticity become more evident **[73]**. These results, together with our findings, strongly suggest that the loss of cortical plasticity is strictly associated with the progression of neurological dysfunction in humans as well. They also add new evidence supporting the idea that the deficit of MeCP2 impairs functional synaptic plasticity in the maturing nervous system and not during brain development.

Importantly, growing consensus suggests the role of inhibitory circuits in regulating human motor cortical plasticity **[77,79]**. Therefore, in RTT, defects in cortical inhibitory connectivity might also explain alteration in motor plasticity. Investigators recently demonstrated that altered activity and connectivity of GABAergic PV interneurons impaired structural and functional plasticity in M1. Specifically, Mecp2 knockout mice displayed an atypical upregulation of PV interneurons in M1 that was associated with the severity of motor behavioral impairments **[41]**. In addition, consistent with a reduction in inhibition received by pyramidal neurons, monocular deprivation induced an abnormally prolonged plasticity in visual cortex of Mecp2+/− female mice **[50, 51, 52]**. Similarly, parvalbumin-specific deletion in mice led to immature adult visual cortical plasticity,5 which was restored by enhancing inhibition via intracerebral infusion of diazepam, a GABAA receptor agonist **[80]**. Importantly, IGF-1, which is considered to play a role in modulating neural plasticity and cortical excitatory transmission in mice,**[39]** was within the normal values in RTT patients and did not correlate with our neurophysiological metrics. These findings are in line with clinical trials on the therapeutic use of IGF-1 in RTT patients, showing normal serum and cerebrospinal fluid levels of IGF-1 before treatment **[52,54]**.

Conclusions and Outlook

Abnormal cortical synaptic plasticity and E/I balance seem to be a prominent feature of RTT and a range of related neurodevelopmental disorders. Dysfunction of GABAergic signaling can be

considered as the common thread underlying cortical abnormalities and associated symptoms **[80, 81]**.

Here we have shown the relationship between motor symptom severity and alteration of neurophysiological metrics of M1. This association raises the possibility of using some neurophysiological parameters as a biomarker of disease progression or to monitor the efficacy of new therapeutic interventions. For instance, LICI, which is a short paradigm (ie, around 5 minutes to accomplish), was a very sensitive metric, being highly associated with motor deficit, and was easy to perform **[85]**.

In addition, because severity of symptoms, including motor dysfunction, is particularly high in late childhood and adolescence, **[82]** the concomitant use of drugs and nonpharmacological therapies such as non invasive brain stimulation protocols (ie, rTMS or transcranial direct current stimulation) for overcoming decreased plasticity or altered E/I balance in M1 seems to be compelling. Important seminal work in RTT animal models showed the possibility of achieving prolonged survival and reversibility of disease phenotypes with gene reinstatement, even into adulthood. These results seemingly make RTT one of the more tractable neurodevelopmental disorders as far as potential for disease modification and improvement **[74, 75, 84]**.

CLINICAL SETTING: A MAGNETOENCEPHALOGRAPHIC STUDY OF NETWORK CONNECTIVITY IN PATIENTS WITH RETT SYNDROME

1. Introduction

Several studies have demonstrated atypical activation and functional connectivity of the inhibition brain network in the RTT. Given the difficulty to study the population with RTT in vivo, poor information comes from studies on autistic subjects or other neurodevelopmental disorders. One way to examine circuit-level changes is with the use of electroencephalography (EEG). Previous studies of the EEG in individuals with RTT have explored spectral power, including power as an index of brain function or disease severity **[86]**. This study suggested that girls with RTT have significantly lower power in the middle frequency band, across multiple brain regions. Additionally, girls with Rett syndrome that are "postregression" demonstrate significantly higher power in the lower frequency delta and theta bands and a significantly more negative slope of the power spectrum. Increased power in these bands trended with lower cognitive assessment scores **[86]**. Increased power in lower frequency bands is consistent with studies demonstrating a "slowing" of the background EEG in Rett syndrome. This increase, particularly in the delta band, could represent abnormal cortical inhibition due to dysfunctional GABAergic signaling and could potentially be used as a marker of severity due to associations with more severe RTT phenotypes **[86]**. Over the years, our teams **[87]** has studied a group of girls with RTT, using magnetoencephalography (MEG). We based our analyses on source-reconstructed MEG data acquired during resting state.

2. Methods

Participants and Clinical Assessment Participants were recruited from the Department of Translational Medical Sciences, Child Neuropsychiatry in "Federico II" University of Naples, Italy. We studied 10 female patients with clinical diagnosis of RTT (age 24.30 +/- 8 years) based on the Neul revised criteria **[14]** and confirmed by mutation in the MECP2 gene, and 10 healthy female individuals (HS) (age 26.10 +/- 6.84 years). This study complied with the Declaration of Helsinki and was approved by the local ethics committee. Written informed consent has been granted by all participants (or their legal guardians).

Acquisition

The data were acquired using a MEG system equipped by 163 magnetometers SQUID (Superconducting Quantum Interference Device) **[88]**, placed in a magnetically shielded room (AtB Biomag, Ulm, Germany), in order to reduce the external noise. Of all squids, 154 are positioned to be as close as possible to the head of the subject, while the remaining ones are more distant so as to measure environmental noise (reference magnetometers). All the subjects of each group underwent a 7-min resting-state MEG acquisition with open eyes, divided in two segments. To evaluate the right position of the head under the helmet, we used Fastrak (Polhemus R) to acquire the position of four coils (attached to the head) and of four anatomical landmarks (nasion, right and left pre-auricular points, and vertex of the head). Before each acquisition segment, the head position in the helmet was obtained. During the acquisition, two electrodes for the electrocardiogram and two for the electrooculogram **[89]** were also acquired.

Figure 1: Data analysis pipeline. (A) Raw magnetoencephalography (MEG) signals recorded by 154 sensors (a subset displayed here). (B–D) Respectively noisy channel, cardiac artifact, blinking artifact, removed during preprocessing phase. (E) MEG signals after artifact removal and noise cleaning. (F) Coregistration between MEG signals and MRI template. (G) Source reconstruction (beamforming). (H) A sequence of four neuronal avalanches. (I) How to calculate the dimension of a neuronal avalanche, in particular, the first (in red square) of the (H) image.

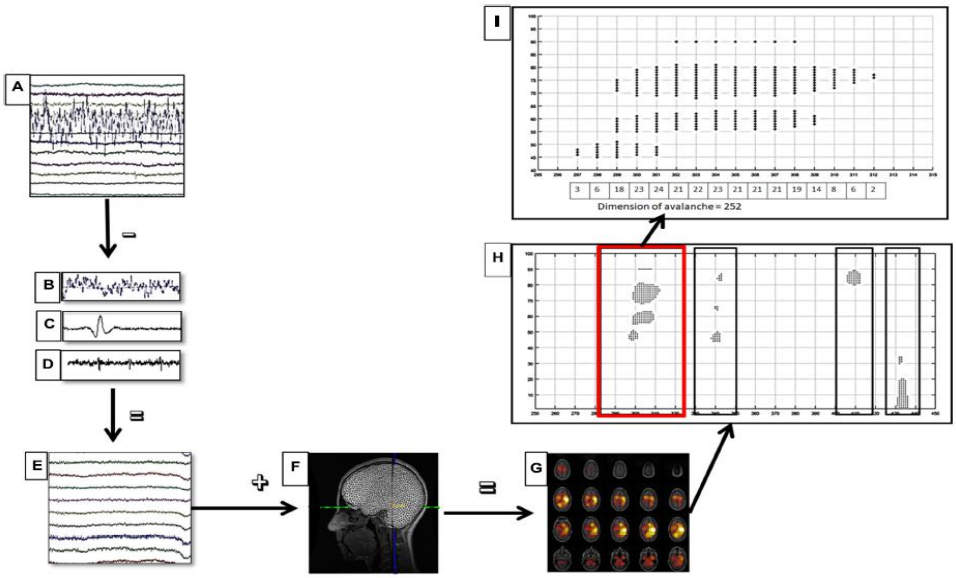

TABLE 3: To appreciate the robustness of the results presented, we reported the variance values around the branching parameters, for RTT patients and HS group, when dataset is split in three segments.

	Segment 1/3		Segment 2/3		Segment 3/3	
	RTT patients	HS	RTT patients	HS	RTT patients	HS
Delta band (Δt = 5)	1.030 (0.010)	1.020 (0.005)	1.033 (0.004)	1.016 (0.009)	1.029 (0.005)	1.011 (0.002)
Alpha band (Δt = 1)	0.971 (0.002)	0.966 (0.001)	0.974 (0.001)	0.961 (0.000)	0.976 (0.001)	0.965 (0.001)
Broadband (Δt = 2)	1.018 (0.001)	1.040 (0.002)	1.020 (0.002)	1.046 (0.001)	1.024 (0.001)	1.043 (0.002)

FIGURE 2: Size distributions of avalanches with the relative power law fitted, for each RTT patient (first line) and for each HS (second line). The colored lines represent the size distributions of avalanches for each subject (RTT patients in the top row, Healthy Subjects in the bottom row). The black bold lines represent the fitted power laws. For brevity, we reported only Delta (1t = 5), Alpha (1t = 1) and Broad (1t = 2) bands. Specifically, the Delta band and the Broad band reached statistical significance, whereas the Alpha band was reported for comparison, as an example, as it does not reach significance (such as Theta, Beta and Gamma). The reported results refer to the threshold SD = 3.

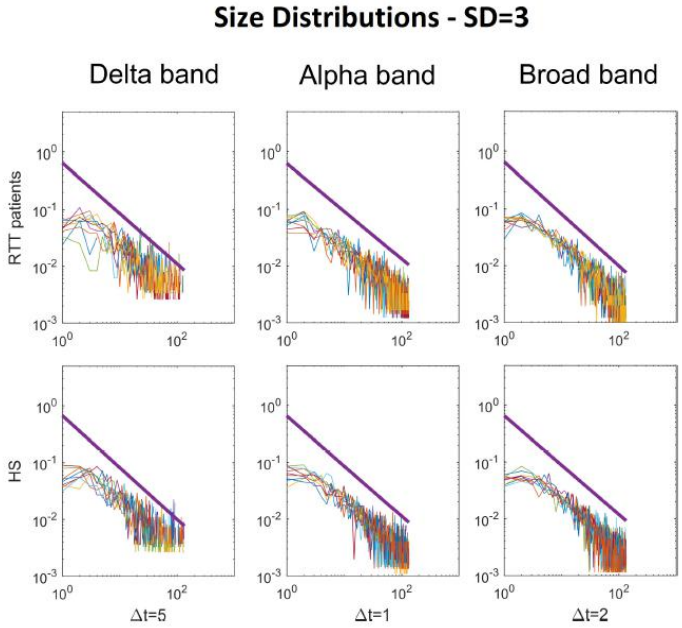

FIGURE 3: Avalanche duration distributions for each RTT patient (first line) and for each HS (second line) for Delta (1t = 5), Alpha (1t = 1) and Broad (1t = 2) bands (the threshold chosen is SD = 3). The blue lines represent the avalanche duration distributions for each subject (RTT patients in the top row, Healthy Subjects in the bottom row). The red lines represent the sum of the avalanche duration distributions across all subjects.

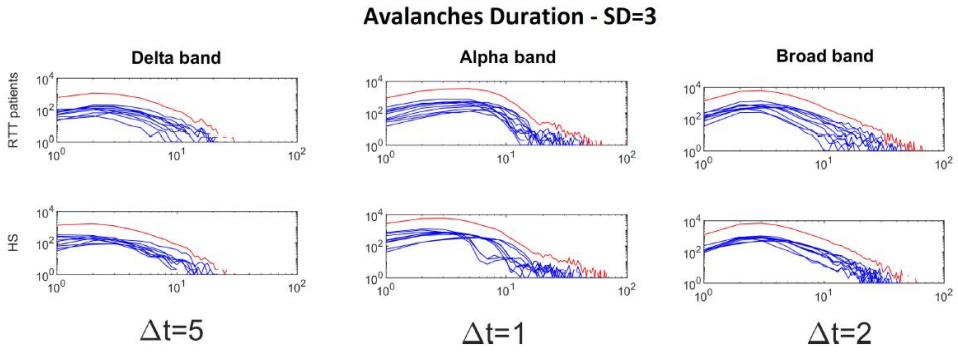

FIGURE 4: Size versus duration for each RTT patient (first line) and for each HS (second line) for delta (1t = 5), alpha (1t = 1), and broad (1t = 2) bands (the threshold chosen is SD = 3).

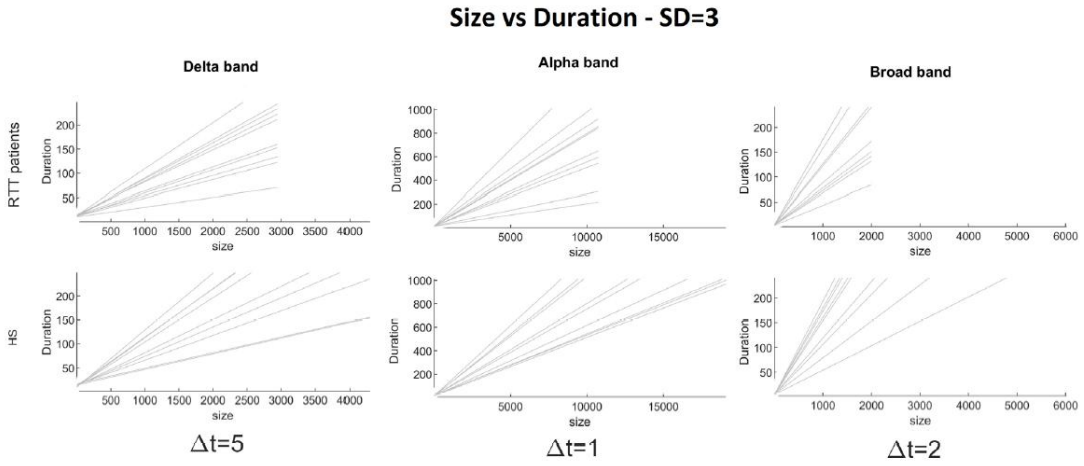

Preprocessing

As previously described (Jacini et al., 2018; Rucco et al., 2019), the MEG signals, after an anti aliasing filter, were acquired with a sampling frequency of 1,024 Hz. A fourth-order Butterworth IIR band-pass filter in the 0.5- to 100-Hz band was subsequently applied to the acquired signals. Environmental noise, measured by reference magnetometers, was removed by using the principal component analysis. MEG data were cleaned of physiological artifacts, such as eye blinking and heart activity, by means of independent component analysis (Sorriso et al., 2019). Visual inspection was used for identification of noisy channels. For all the preprocessing steps, we used the FieldTrip toolbox (Oostenveld et al., 2011).

Source Reconstruction

Time series of neuronal activity were reconstructed in 116 regions of interests (ROIs) based on the automated anatomical labeling (AAL) atlas (Tzourio-Mazoyer et al., 2002) using a linearly constrained minimum variance beam-former algorithm (Van Veen et al., 1997; Nolte, 2003) based on MRI template and then filtered both in broadband (0.5– 48 Hz) and in the five classical frequency bands [delta (0.5–4.0 Hz), theta (4.0–8.0 Hz), alpha (8.0–13.0 Hz), beta (13.0–30.0 Hz), and gamma (30.0–48.0 Hz)]. From the 116 ROIs of the AAL Atlas, we have excluded 26 ROIs corresponding to the cerebellum because of their low reliability in MEG (Lardone et al., 2018). Hence, we considered a total of 90 ROIs. We have resampled the source-space time series at 512 Hz.

FIGURE 5: Average size distributions for both groups, for Delta (1t = 5), Alpha (1t = 1) and Broad (1t = 2) bands, as a function of the threshold (from 1 to 3 SD). The blue lines represent the average of the avalanche size distributions across either the RTT patients or the HS (as indicated in the y-label). The red lines represent the fitted power law.

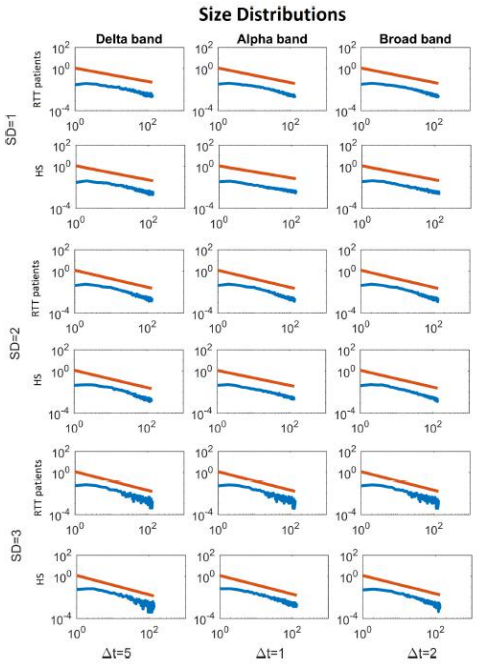

FIGURE 6: Avalanches duration distributions for both groups for Delta (1t = 5), Alpha (1t = 1) and Broad (1t = 2) bands as a function of the threshold (from 1 to 3 SD). The blue lines represent the avalanche duration distributions across either the RTT patients or the HS (as indicated in the y-label). The red lines represent the sum of the avalanche duration distributions across all subjects.

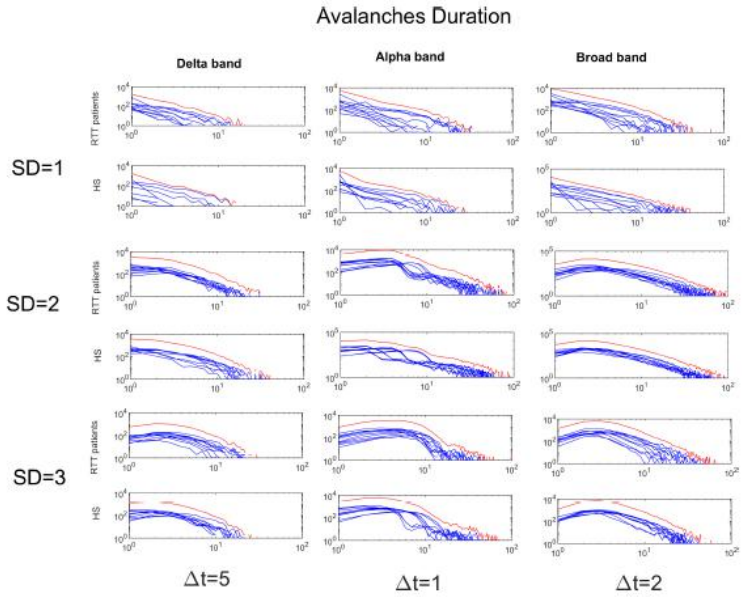

Signal Discretization

For each ROI, the time series were discretized with five different time bin durations Δt, each one multiple of Δtmin (19 ms), corresponding to the sampling period. An event was identified by a positive or a negative excursion of an area, in a bin, beyond a threshold, defined as +/-3 SD of the signal amplitude, which was a tradeoff between a lower threshold (leading to the detection of more spurious noise events in addition to real ones) and a higher threshold (missing real events). Indeed, MEG systems rely on squid sensors, which measure the magnetic field generated by brain activity. However, such sensors cannot identify the field direction. For this reason, both positive and negative excursions were picked up without distinction. As a result, the event was identified when the absolute value of this excursion exceeded the chosen threshold.

Branching Parameter

As previously described (Beggs and Plenz, 2003; Shriki et al., 2013), an avalanche is defined as a sequence of contiguous time bins starting when at least one ROI is active and ending when all regions are inactive. The number of events in all ROIs in an avalanche corresponds to its size. For each subject and for each time bin size, the branching parameter s was estimated by calculating, for each avalanche, the averaged (over all the time bins) ratio of the number of events between the subsequent time bin (descendants) and that in the current time bin (ancestors), and then averaging it over all the cascades (Bak et al., 1987). More specifically:

$$\sigma = \frac{1}{N_{aval}} \sum_{i=1}^{N_{aval}} \sigma_i$$

$$\sigma_i = \frac{1}{N_{bin} - 1} \sum_{j=1}^{N_{bin}-1} \frac{n_{events}\,(j+1)}{n_{events}\,(j)}$$

Statistical Analysis

We compared the distribution parameter a in patients and controls using permutation testing (Nichols and Holmes, 2002), for each frequency band. Specifically, at each iteration, each subject is randomly assigned to one of the two groups and then the difference between the averages of the two groups was computed. The group assignment is permuted 104 times, obtaining the null distribution of group differences, which was used to define the statistical significance of the observed difference between patients and controls. All the analyses were performed at a significance level of 0.05, using Matlab R2017a (MathWorks R) environment.

3. Results

As described in the Methods section, we discretized the ROI signals as a train of events, each of them representing the signal exceeding the threshold of +/-3 SD. First, we checked the critical condition in both groups, in all frequency bands, for all time bins. We found, for both groups, a branching parameter σ=1, in delta band for bin $\Delta t = 5$, in theta and alpha band for bin $\Delta t = 1$, in beta-, gamma-, and broadband for bin $\Delta t = 2$, as reported in **Table 1**. Moreover, to demonstrate the robustness of the estimation of the branching parameter, we estimated the variance around sigma both when we split our dataset into two segments (**Table 2**) and when we divided it into three segments (**Table 3**). To demonstrate the strength of our data, we reported, for the chosen threshold SD = 3, the size distribution fitted with a power law (**Figure 2**), duration distributions (**Figure 3**), and average size versus duration distributions (**Figure 4**) for each subject, in all time bins, for both groups separately (for brevity, we reported only delta, alpha, and broadbands). Again, we provided the effect of different thresholds (1 to 3 SD) on our data in size distributions (**Figure 5**), duration distribution (**Figure 6**), and average size versus duration distributions (**Figure 7**).

Furthermore, to test that our results might not be biased by spatial subsampling, we demonstrate the presence of scale time separation (Levina and Priesemann, 2017), as reported in **Figure 8**.

Last, to quantify the robustness of power law fitting, we evaluated the ECDF of HD for both groups, for all time bins in delta, alpha, and broadbands, and as reported in **Figure 9**, the highest HD is less than 0.3. Finally, a comparison of the a parameter between both groups was carried out, highlighting significant differences in the delta band ($p = 0.0423$) and in broadband ($p = 0.0174$), as shown in **Figure 10**. In particular, RTT patients invariably showed a lower distribution parameter a in both frequency bands, for all time bins. No significant differences were found in other frequency band. law (**Figure 2**), duration distributions (**Figure 3**), and average size versus duration distributions (**Figure 4**) for each subject, in all time bins, for both groups separately (for brevity, we reported only delta, alpha, and broadbands). Again, we provided the effect of different thresholds (1 to 3 SD) on our data in size distributions (**Figure 5**), duration distribution (**Figure 6**), and average size versus duration distributions (**Figure 7**). Furthermore, to test that our results might not be biased by spatial subsampling, we demonstrate the presence of scale time separation (Levina and Priesemann, 2017), as reported in **Figure 8**. Last, to quantify the robustness of power law fitting, we evaluated the ECDF of HD for both groups, for all time bins in delta, alpha, and broadbands, and as reported in Figure 9, the highest HD is less than 0.3.

Finally, a comparison of the a parameter between both groups was carried out, highlighting significant differences in the delta band ($p = 0.0423$) and in broadband ($p = 0.0174$), as shown in **Figure 10**. In particular, RTT patients invariably showed a lower distribution parameter a in both frequency bands, for all time bins. No significant differences were found in other frequency bands.

FIGURE 7: Size versus duration for both groups for delta (1t = 5), alpha (1t = 1), and broad (1t = 2) bands varying the threshold (1 to 3 SD).

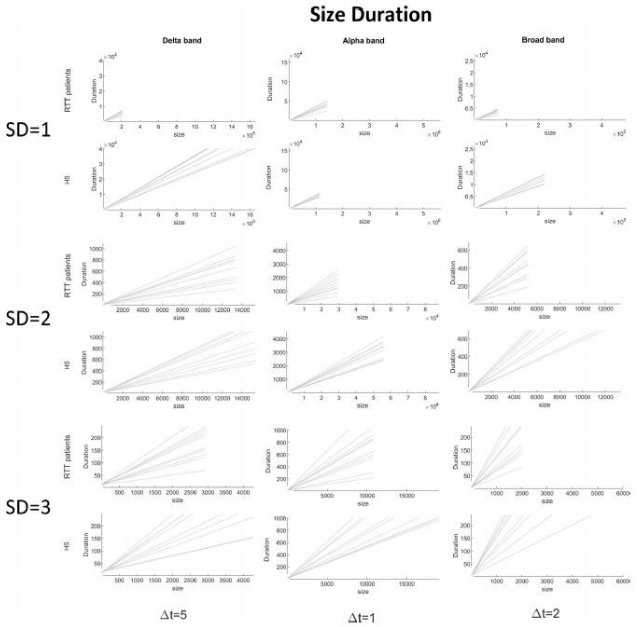

FIGURE 8: Duration versus pause for both groups for delta (1t = 5), alpha (1t = 1), and broad (1t = 2) bands varying the threshold (1 to 3 SD).

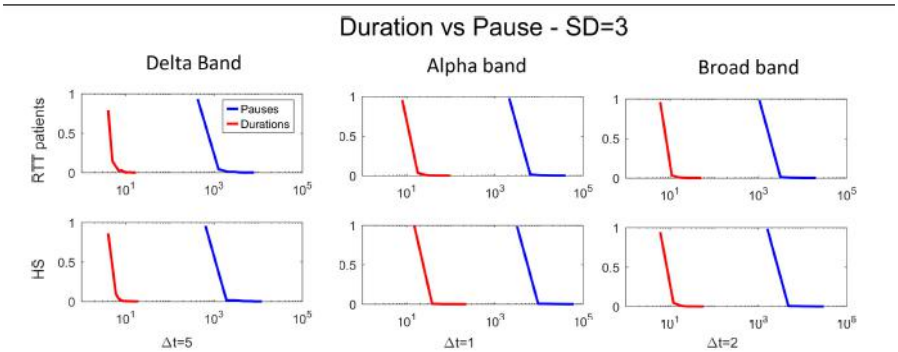

FIGURE 9: The empirical cumulative distribution functions of the Hellinger distance for RTT patients and HS separately, in all time bins, for delta, alpha, and broadbands. The chosen threshold is SD = 3.

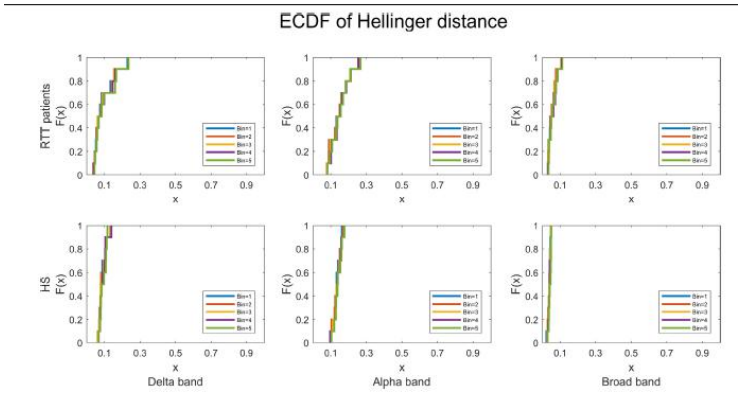

FIGURE 10: Comparison of a parameter in broadband for time bin 1t = 2 and in delta band for time bin 1t = 5 between RTT patients (blue dots) and HS (red dots).

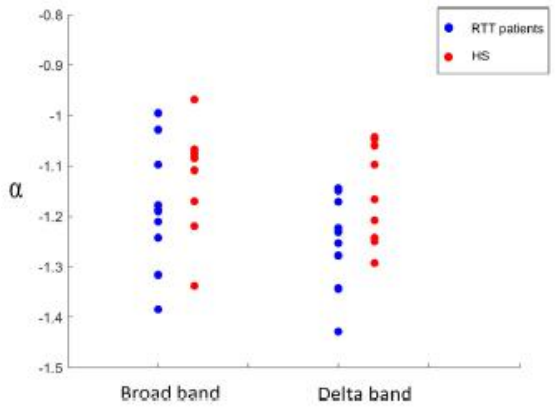

5. Discussion

In this work, we set out to test the hypothesis that genetic mutations related to RTT would induce a reorganization of the whole-brain activity. In particular, we characterized the distribution of neuronal avalanches in a group of 10 patients with Rett syndrome and 10 matched controls, using MEG, in an open-eye resting-state condition. The analysis was performed both in broadband and in the five canonical frequency bands. The study originated from recent evidence showing that the dynamics of resting-state brain activity, measured using MEG, produces scale-invariant neuronal avalanches, suggesting that the critical state is a physiological condition that is (presumably) optimal to the brain functioning. Consequently, the deviations from this optimally tuned configuration might convey the effects of the disease on large-scale coordinated activity (Meisel et al., 2012).

Our data are in line with recent findings showing that, in humans, the dynamics of resting-state brain activity is well described by a branching process where the sigma parameter is close to 1 (Meisel et al., 2013; Shriki et al., 2013). Besides these confirmatory results, the main goal of this work is to study the frequency-specific differences in functional dynamics in RTT patients with respect to a control group. Our data showed that, around the critical state, the distribution size of neuronal avalanches, for both groups, obeys a power law. Interestingly, RTT patients show a lower value of the distribution parameter a both in delta and broadband, compared to controls. Furthermore, the exponents of the power law distributions vary greatly per each frequency band. This result is in line with Thompson et al., which suggests that resting-state connectivity is a frequency-dependent phenomenon (Thompson and Fransson, 2015).

The aforementioned results collectively suggest a global rearrangement in the brain functional dynamics of Rett patients. In fact, big avalanches capture the presence of widespread coordinated activations, with many different brain areas activating in a complex, meaningful sequence. The lack of large avalanches in patients might be a sign of the inability of the brain to coordinate a sufficient number of areas in sequence. One might speculate that the lack of large patterns of structured activity might be capturing the effects of the circuital changes induced by the genetic mutations present in RTT. This hypothesis might be compatible with the work by Armstrong et al., which claims that whole-brain structural changes are related to small, low-density neurons that have less dendritic branching and spine density (Armstrong et al., 1995). Furthermore, in the RTT syndrome, the dendrites of pyramidal neurons in the motor and frontal cortices are considerably shorter than in HS (Armstrong et al., 1995).

Concluding, in our study we analyzed brain dynamics during eye-open resting state, measuring the size distribution of neuronal avalanches. We found a lower distribution parameter a in RTT patients in the delta frequency band and in the broadband, compared to controls. Such finding means that patients display a larger number of small avalanches and a lower number of big avalanches. These results can be explained in terms of reduced long-range coordination of neuronal activity across the brain in the pathological group. Such altered brain dynamics is likely to be suboptimal, and might underpin some of the symptomatology observed in RTT. Additionally, our results suggest that neuronal avalanches could be an innovative and advanced method to study the dynamics of brain activity. In fact, despite the rising interest in what constitutes the normal cortical dynamics in healthy humans, the nature of the alterations induced by pathological processes remains a major question in neuroscience. Interestingly, the observation that cortical networks optimize information processing when they are in a critical state might be exploited to identify subtle, preclinical brain dysfunction. Furthermore, the study of the critical dynamics of the human brain could be enhanced by comparing normal resting avalanches with evoked states or pharmacologically modified states and assessing the sensitivity (or performing a profile analysis) of the system with respect to the branching parameter values. Finally, such approaches are inherently multivariate, taking into account the activity of all brain areas at once, hence providing solid theoretical ground to the study of emerging, holistic properties of the brain.

FUTURE PERSPECTIVES: VALIDATION OF A NEW NEUROPHYSIOLOGICAL BIOMARKER OF MOTOR DISABILITY IN PATIENTS WITH RETT SYNDROME: AN INNOVATIVE COMBINED NEUROPHYSIOLOGY AND PHYSICAL THERAPY PROTOCOL TO ENHANCE CORTICAL PLASTICITY

Transcranial magnetic stimulation (TMS) was used to probe cortical plasticity in people with RTT. TMS activates human motor cortex transcranially; specifically, according to the microcircuit model TMS induces strong depolarization of layer II/III pyramidal and inhibitory cells that in turns leads to highly synchronized recruitment of clusters of excitatory neurons, including pyramidal neurons of layer V, that represent the major output of M1 [45]. By using ad hoc protocols of paired pulse TMS and repetitive TMS we demonstrated alteration of cortical excitability balance within M1, but more interestingly we showed the reduction of motor cortex plasticity in RTT patients and such impairment was strictly correlated to motor deficit, indexed by motor clinical severity scales. Importantly, as ancillary investigation we assessed the serum level of insulin-like growth factor 1 (IGF1), implicated in the mechanisms of cortical plasticity, and we did not find any specific abnormalities in our RTT sample. The relationship we found between motor symptoms severity and alteration of neurophysiological metric of M1 plasticity raises the possibility of using this neurophysiological parameter as a biomarker of disease progression or to monitor the efficacy of new therapeutic interventions.

Importantly, over the last years, the impairment of motor cortex plasticity, underlying some neurological diseases, has been successfully modulated by combining motor and or cognitive training with non-invasive brain stimulation techniques (NIBS), such as transcranial direct current stimulation (tDCS). tDCS has been shown to modulate cognitive functions in healthy humans, and to alter psychiatric and neurological symptoms in patients via induction of plasticity [90]. tDCS induces polarity-dependent neuroplastic changes in the brain, which can last for hours depending on the dosage of stimulation. In the primary motor cortex, an enhancement of cortical excitability is observed when the anode is placed over the target region with stimulation intensities for up to 2 mA, and stimulation durations for up to 20 min, and an excitability reduction with the cathode over the target region for a stimulation intensity of 1 mA and an electrode size of 35 cm^2 . Unlike other NIBS techniques, such as repetitive TMS, tDCS uses weak direct currents to induce gradual changes of the resting membrane potential of cortical neurons in a polarity dependent manner – anodal stimulation leads to a subthreshold depolarization whereas cathodal stimulation leads to hyperpolarization of neuronal compartments critical for the respective excitability, and neuronal activity alterations. Afterwards, multiple effects of tDCS applied over different brain areas have been described in humans and modulation of brain plasticity has been suggested to account for tDCS after-effects lasting days or weeks [90]. There is also evidence supporting the use of tDCS when combined with traditional rehabilitative techniques in patients with neurological, motor, cognitive, and language disorders. For instance, tDCS of motor cortex alone or in combination with intensive physical therapy has been used for the treatment of movement disorders, including dystonia, Parkinson's disease and stroke [91]. Due to these positive findings, the current methodological direction is to involve functional targeting in tDCS studies aimed at enhancing the effects of a particular training program by combining it with tDCS. Although this combined approach is attracting considerable interest in the multiple disability area, due to positive results, it has not been widely applied to neurodevelopmental disorders, such as RTT.

The work of Fabio et al. [92] is the first study designed to examine the neurophysiological and cognitive effects of tDCS in girls with RTT with chronic language impairments. The authors applied an integrated intervention: tDCS and cognitive empowerment applied to language to enhance speech production (new functional sounds and new words). Because maximal gains are

usually achieved when tDCS is coupled with behavioural training, they applied tDCS stimulation on Broca's area together with linguistic training. The results indicated a general enhancement in language abilities, motor coordination, and neurophysiological parameters (an increase in the frequency and power of alpha, beta and theta bands at EEG). A subsequent study of the same group [93] combined traditional cognitive training with anodal tDCS applied over the left motor cortex (M1) to improve attention and language abilities. The results of this study indicated longer attention time in the active tDCS group compared to the sham tDCS group with a stable trend also in the follow-up phase; an increase of the number of vowel/phonemes sounds in the active tDCS group and an improvement in the EEG parameters, mainly alfa and beta bands, in the active tDCS group. Overall, these preliminary results are encouraging and indicate that a combined protocol can help subjects with RTT maximize their capacities. For these reasons, the use of tDCS with rehabilitation can be a valid and safe treatment.

As for rehabilitation, a recent review of our group [94] emphasized that a multimodal individualized physical therapy program should be regularly recommended to patients with RTT syndrome in order to preserve autonomy and to improve quality of life. For instance, environmental enrichment (EE) is a very promising rehabilitation therapy. It is based on the stimulation of the brain by its physical and social surroundings. Brains in richer, more stimulating environments have higher rates of synaptogenesis and more complex dendrite arbors, leading to increased brain neuroplasticity. This effect takes place primarily during neurodevelopment, but also during adulthood to a lesser degree. A recent study has demonstrated that EE can reduce functional deficit in RTT and this beneficial effect is associated with a threefold increase in serum Brain-derived neurotrophic factor (BDNF) levels alongside parallel gains in gross motor skills [58]. This result is in line with preclinical models where EE at presymptomatic stages (postnatal day 28) caused an improvement of motor coordination in female Mecp2 heterozygous mice. Interestingly, brain BDNF levels correlated with the improvement of motor performance. BDNF is a protein required for many aspects of neuronal development, as well as synaptic transmission and plasticity. There is some clinical evidence of a role for BDNF in Rett syndrome pathogenesis. Two studies described lower Bdnf mRNA levels in autopsy brain samples from RTT individuals, which is reminiscent of the situation in Mecp2 mutant mice.

Both, BDNF and tDCS are implicated in cortical plasticity and several studies have demonstrated a strict relationship between the effectiveness of plasticity induced effect of tDCS and the level of BDNF. Indeed, preclinical studies have demonstrated that anodal tDCS can induce an up-regulation of expression of BDNF exons and therefore protein levels.

In this complex scenario, our project seeks to address several questions.

Is cortical plasticity a possible and reliable biomarker of disease severity and progression in RTT patients?

If yes, can our neurophysiological biomarker be used as surrogate of such defective cortical plasticity?

Lastly, by using an innovative protocol based on the combination of tDCS with physical therapy, can we really boost cortical plasticity and possibly get an improvement of clinical and laboratory parameters in our patients?

The results of this study could have high impact for the research community since the introduction of a precise, easy to perform and non- invasive biomarker of motor deficit could be used as a measure to evaluate the efficacy of future treatments.

Indeed, in the RETT community there is the need of minimally invasive and accurate biomarkers of disease progression and treatment response that could facilitate screening of therapeutic compounds, the enrolment of better-defined participants into clinical trials, and treatment monitoring. Interestingly, since severity of symptoms, including motor dysfunction, is particularly

high in late childhood and adolescence, the concomitant use of non-pharmacological therapies, such as non-invasive brain stimulation protocols (i.e. transcranial direct current stimulation) for overcoming decreased plasticity in motor cortex seems to be compelling. Important seminal work in Rett syndrome animal models showed the possibility to achieve prolonged survival and reversibility of disease phenotypes with gene reinstatement, even into adulthood. These results seemingly make Rett syndrome one of the more tractable neurodevelopmental disorders as far as potential for disease modification and improvement.

OBJECTIVES

Our overarching hypothesis is that our neurophysiological biomarker of cortical plasticity is a reliable and objective biomarker of motor impairment severity that can predict in the long run disease progression. We postulate that this new biomarker is dynamically influenced by external treatment boosting cortical plasticity such as environmental enrichment and transcranial direct current stimulation. Based on our recently published study, we predict that our motor cortex plasticity biomarker should be associated to motor deficit and that after the combination of tDCS with motor training we should get an improvement of motor performance that parallels with the level of motor cortex plasticity, such improvement should be more evident in the active group respect to the sham one. Motor improvement and the gain of cortical plasticity should be paralleled by the increase of BDNF levels. In the long run, we also predict that patients with low level of our neurophysiological biomarker and/or "non responders" to induced plasticity protocols, should exhibit a poor disease prognosis.

RESEARCH DESIGN and METHODOLOGY

A schematic representation of our research design is showed in Figure 1.

Experimental plan

This will be a double-blind, randomized (1:1), sham-controlled, single-center trial. The study will enroll 30 RTT patients (age range: 14-30 years) with a mild to severe phenotype, in an interval of 16 weeks. Anodal tDCS will be delivered during five consecutive days for two weeks. Fifteen patients will receive anodal tDCS plus environmental enrichment and fifteen sham stimulation plus environmental enrichment in randomized order (figure 1). We estimate that 15 individuals per group to be large enough to secure a sufficient statistical power > 0.8, for medium effect sizes. The Rett syndrome gross motor scale (RSGMS) score of the screening visit will be used as stratification variables. According to our recent study (Bernardo et al., 2020) and to previous literature, antiepileptic drugs should not affect neurophysiological cortical plasticity parameter.

Intervention: tDCS and Environmental enrichment

Anodal tDCS will be delivered by two 7 × 5 cm surface rubber electrodes, which are connected to a battery-driven constant-current stimulator (Eldith-NeuroConn GmbH, Ilmenau, Germany). Anodal tDCS (2mA intensity for 20 min once a day for five consecutive days for two weeks) will be transferred by a pair of saline-soaked surface sponge electrodes (35 cm^2) positioned over the left primary motor cortex (anode) and over the contralateral supraorbital area (cathode). For sham tDCS, the current will be ramped up to 2mA and slowly decreased over 30 s to ensure the typical initial tingling sensation. Anode electrode will be placed on the motor hot spot of the first interosseous muscle (FDI) elicited by transcranial magnetic stimulation.

Just after each daily stimulation protocol, patients will undergo Environmental enrichment will include multiple supported activities selected to target individual goals in the development of motor

skills and endurance. Activities will focus particularly on balance and walking and included a high volume of practice aiming to increase BDNF production and boost cortical plasticity. The intervention will also be consistent with Motor Learning Theory, including opportunities for practice, intrinsic and extrinsic feedback, judicious use of rest periods, and performance of tasks in a variety of conditions that provide choice. Each motor activity will be supplemented with visual, auditory, taste, vestibular and tactile stimulation to build the richness of the sensory-motor environment (Fig. 1). The intervention will be conducted for 2 to 3 h on five mornings per week for two weeks with one-on-one supervision provided by a physiotherapist at our University hospital.

Outcomes measures

Neurophysiological assessment of cortical plasticity by TMS

Repetitive TMS (rTMS) evaluates long term potentiation (LTP)-like activity of central motor circuits and thus, can reveal abnormalities in brain plasticity. Herein, we will use patterned rTMS, namely intermittent theta burst stimulation (iTBS), to investigate LTP within M1. Intermittent theta burst stimulation (iTBS) will be applied by using the well-known paradigm introduced by Huang and colleagues (2005). It will be consisted in bursts of three pulses at high frequency, 50 Hz, repeated at intervals of 200 ms, delivered in short trains lasting 2 s, with an 8 s pause between consecutive trains, for a total number of 600 pulses. The stimulation intensity for iTBS will be set at 80% of active motor threshold.

To assess cortico-spinal excitability before iTBS, single MEPs will be recorded using a stimulus intensity adjusted to produce MEP amplitude of approximately 0.5 mV in the relaxed FDI muscle. For each subject, 20 MEPs will be recorded, and the peak-to-peak amplitudes will be measured to calculate the mean amplitude.

After the interventions, cortico-spinal excitability changes will be monitored by collecting 12 MEP responses (0.2 ± 10% Hz) every 2 minutes following the intervention for up to 30 min (15 blocks, starting with 2 min of rest, then 1 min measurement, 1 min rest, and so on. We decided to adopt a high temporal resolution of cortico-spinal excitability assessment after iTBS for a better estimation of the different patterns of motor cortex plasticity across the groups over time.

Figure 1. Schematic overview of research project

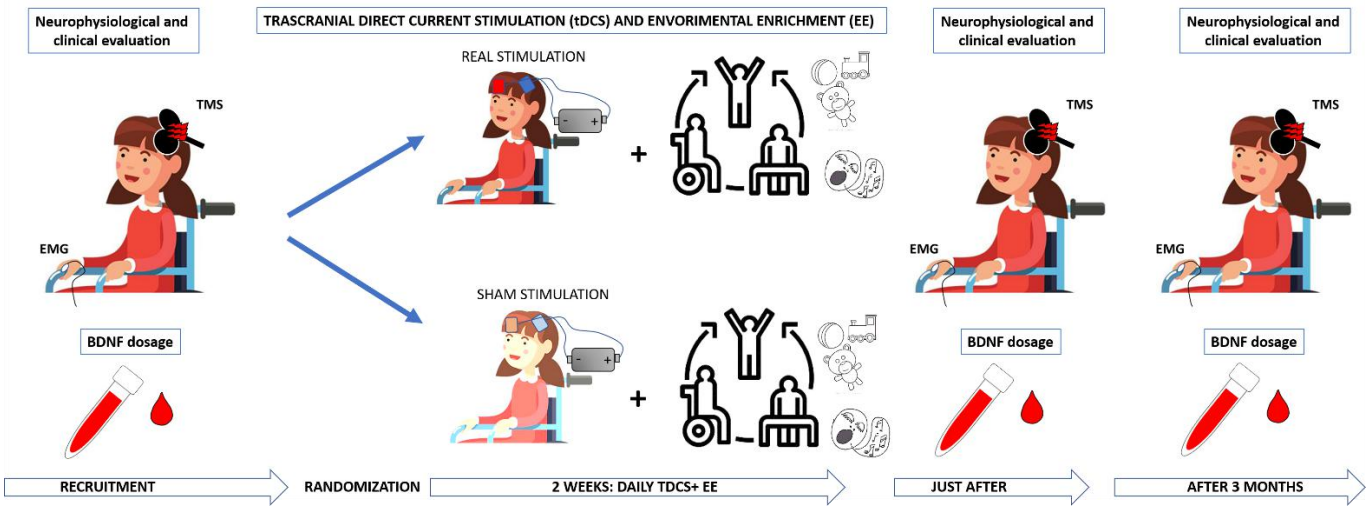

Clinical evaluation of motor abilities at baseline and over the time

All participants will undergo extensive clinical evaluation, with special focus on motor abilities. Specifically, a child neuropsychiatrist with expertise in RTT syndrome will administered the Rett Syndrome Gross Motor Scale (RSGMS). The RSGMS comprises 15 items for sitting, standing, walking, and transition activities rated according to the observed level of assistance (no assistance, mild, moderate, or maximal assistance/unable) and using a 0 to 3 scale with 3 representing better function. The scale has demonstrated strong internal consistency, expected relationships between scores, age and genotype, excellent test-retest reliability, and an observed difference of four points in an individual would represent change beyond within-subject error. In addition, our neurophysiological biomarker is strictly associated to RSGMS [85]. A blinded assessor will code the gross motor skills. Gross motor data will be collected at baseline period, just after the intervention period and after three months. Clinical outcome measures will be then correlated with our neurophysiological and laboratory biomarkers.

Serum level of BDNF

For each RTT patient, we will evaluate serum level of BDNF. Blood samples will be taken at the beginning and end of the stimulation and EE protocol and then again after the three-month intervention period. For each test, blood will be taken in the afternoon after lunch to standardise the time of day and relation with food intake. Samples will be collected in anticoagulant tubes and stored at −80 degrees C. At the time of testing, the whole blood will be lysed with 3% triton X-100 (Amresco, Ohio) with sonification for 5 s for 20 times with a 10-s interval between each disruption (Scientz98-III, Scientz Biotechnology Co Ltd., Ningbo). Disrupted cell membranes will be discarded by centrifuging the samples at 2000 g for 15 min at 4 °C. The supernatant will be aliquoted for storage and the BDNF protein concentration will be measured with commercially available two-site sandwich enzyme-linked immunoabsorbent assay (ELISA) kits (RAYBIOTECH, Norcross GA US; catalogue number ELH-BDNF Lot: 0520160106). Each blood sample will be diluted *100 and tested in triplicate according to the manufacturer's instructions. Mean values of the three concentrations of BDNF (ng/ml) will be used for analysis.

References

1. A. Rett. [über ein eigonartiges hirnatrophisches syndrom bei hyperammonämie im kindesalter. [On a unusual brain atrophy syndrome in hyperammonemia in childhood]] Wiener medizinische Wochenschrift, 116 (1966), pp. 723-726.

2. B. Hagberg, J. Aicardi, K. Dias, O. Ramos. A progressive syndrome of autism, dementia, ataxia, and loss of purposeful hand use in girls: Rett's syndrome: report of 35 cases. Ann Neurol, 14 (1983), pp. 471-479.

3. R.E. Amir, I.B. Van den Veyver, M. Wan, C.Q. Tran, U. Francke, H.Y. Zoghbi Rett syndrome is caused by mutations in X-linked MECP2, encoding methyl-CpG-binding protein 2 Nat Genet, 23 (1999), pp. 185-188.

4. J.D. Lewis, R.R. Meehan, W.J. Henzel, et al. Purification, sequence, and cellular localization of a novel chromosomal protein that binds to methylated DNA Cell, 69 (1992), pp. 905-914.

5. R.J. Klose, A.P. Bird. Genomic DNA methylation: the mark and its mediators Trends Biochem Sci, 31 (2006), pp. 89-97.

6. M. Chahrour, S.Y. Jung, C. Shaw, et al. MeCP2, a key contributor to neurological disease, activates and represses transcription Science, 320 (2008), pp. 1224-1229.

7. P.J. Skene, R.S. Illingworth, S. Webb, et al. Neuronal MeCP2 is expressed at near histone-octamer levels and globally alters the chromatin state Mol Cell, 37 (2010), pp. 457-468

8. N.A. Quaderi, R.R. Meehan, P.H. Tate, et al. Genetic and physical mapping of a gene encoding a methyl CpG binding protein, Mecp2, to the mouse X chromosome Genomics, 22 (1994), pp. 648-651

9. J. Guy, B. Hendrich, M. Holmes, J.E. Martin, A. Bird. A mouse Mecp2-null mutation causes neurological symptoms that mimic Rett syndrome Nat Genet, 27 (2001), pp. 322-326

10. J. Guy, J. Gan, J. Selfridge, S. Cobb, A. Bird. Reversal of neurological defects in a mouse model of Rett syndrome. Science, 315 (2007), pp. 1143-1147

11. R.Z. Chen, S. Akbarian, M. Tudor, R. Jaenisch. Deficiency of methyl-CpG binding protein-2 in CNS neurons results in a Rett-like phenotype in mice. Nat Genet, 27 (2001), pp. 327-331.

12. M. Shahbazian, J. Young, L. Yuva-Paylor. Mice with truncated MeCP2 recapitulate many Rett syndrome features and display hyperacetylation of histone H3. Neuron, 35 (2002), pp. 243-254

13. H.N. Cukier, A.M. Perez, A.L. Collins, Z. Zhou, H.Y. Zoghbi, J. Botas. Genetic modifiers of MeCP2 function in Drosophila. PLoS Genet, 4 (2008), p. e1000179

14. J.L. Neul, W.E. Kaufmann, D.G. Glaze, et al. Rett syndrome: revised diagnostic criteria and nomenclature. Ann Neurol, 68 (2010), pp. 944-950.

15. R.J. Schultz, D.G. Glaze, K.J. Motil, et al. The pattern of growth failure in Rett syndrome. Am J Dis Child, 147 (1993), pp. 633-637

16. Y. Nomura. Early behavior characteristics and sleep disturbance in Rett syndrome. Brain Dev, 27 (Suppl. 1) (2005), pp. S35-S42.

17. P.O. Julu, A.M. Kerr, F. Apartopoulos, et al. Characterisation of breathing and associated central autonomic dysfunction in the Rett disorder. Arch Dis Child, 85 (2001), pp. 29-37

18. L. Jian, L. Nagarajan, N. de Klerk, et al. Predictors of seizure onset in Rett syndrome J Pediatr, 149 (2006), pp. 542-547.

19. A.K. Percy. Rett syndrome: recent research progress. J Child Neurol, 23 (2008), pp. 543-549.

20. R.H. Mount, R.P. Hastings, S. Reilly, H. Cass, T. Charman. Behavioural and emotional features in Rett syndrome. Disabil Rehabil, 23 (2001), pp. 129-138

21. B. Hagberg. Rett syndrome: long-term clinical follow-up experiences over four decades. J Child Neurol, 20 (2005), pp. 722-727.

22. J.M. LaSalle, J. Goldstine, D. Balmer, C.M. Greco. Quantitative localization of heterogeneous methyl-CpG-binding protein 2 (MeCP2) expression phenotypes in normal and Rett syndrome brain by laser scanning cytometry. Hum Mol Genet, 10 (2001), pp. 1729-1740.

23. Z. Zhou, E.J. Hong, S. Cohen, et al. Brain-specific phosphorylation of MeCP2 regulates activity-dependent Bdnf transcription, dendritic growth, and spine maturation. Neuron, 52 (2006), pp. 255-269.

24. P. Moretti, H.Y. Zoghbi. MeCP2 dysfunction in Rett syndrome and related disorders. Curr Opinion Genet Dev, 16 (2006), pp. 276-281.

25. B. Hendrich, A. Bird. Identification and characterization of a family of mammalian methyl-CpG binding proteins. Mol Cell Biol, 18 (1998), pp. 6538-6547.

26. X. Nan, R.R. Meehan, A. Bird. Dissection of the methyl-CpG binding domain from the chromosomal protein MeCP2. Nucleic Acids Res, 21 (1993), pp. 4886-4892

27. A.L. Collins, J.M. Levenson, A.P. Vilaythong, et al. Mild overexpression of MeCP2 causes a progressive neurological disorder in mice. Hum Mol Genet, 13 (2004), pp. 2679-2689

28. K.C. Hoffbuhr, L.M. Moses, M.A. Jerdonek, S. Naidu, E.P. Hoffman. Associations between MeCP2 mutations, X-chromosome inactivation, and phenotype. Ment Retard Dev Disabil Res Rev, 8 (2002), pp. 99-105

29. M. Rastegar, A. Hotta, P. Pasceri, et al.. MECP2 isoform-specific vectors with regulated expression for Rett syndrome gene therapy. PLoS ONE, 4 (2009), p. e6810

30. C. Brendel, E. Klahold, J. Gartner, P. Huppke. Suppression of nonsense mutations in Rett syndrome by aminoglycoside antibiotics. Pediatr Res, 65 (2009), pp. 520-523

31. W.G. Chen, Q. Chang, Y. Lin, et al. Derepression of BDNF transcription involves calcium-dependent phosphorylation of MeCP2. Science, 302 (2003), pp. 885-889

32. N. Nag, J.M. Moriuchi, C.G. Peitzman, B.C. Ward, N.H. Kolodny, J.E. Berger-Sweeney. Environmental enrichment alters locomotor behaviour and ventricular volume in Mecp2 1lox mice. Behav Brain Res, 196 (2009), pp. 44-48

33. N. Rueda, M. Llorens-Martin, J. Florez, et al. Memantine normalizes several phenotypic features in the Ts65Dn mouse model of Down syndrome. J Alzheimers Dis, 21 (2010), pp. 277-290

34. Banerjee A, Miller MT, Li K, Sur M, Kaufmann WE. Towards a better diagnosis and treatment of Rett syndrome: a model synaptic disorder. Brain. 2019 Feb 1;142(2):239-248

35. Jiang M, Ash RT, Baker SA, Suter B, Ferguson A, Park J, et al. Dendritic arborization and spine dynamics are abnormal in the mouse model of MECP2 duplication syndrome. J Neurosci 2013; 19518–33.

36. FY Ismail, A Fatemi, MV Johnston. Cerebral plasticity: Windows of opportunity in the developing brain. Eur J Paediatr Neurol. 2017;21:23-48.

37. Leonard H, Cobb S, Downs J. Clinical and biological progress over 50 years in Rett syndrome. Nat Rev Neurol 2016;13:37–51.

38. Banerjee A, Rikhye RV, Breton-Provencher V, et al. Jointly reduced inhibition and excitation underlies circuit-wide changes in cortical processing in Rett syndrome. Proc Natl Acad Sci U S A 2016;113: E7287–E7296.

39. Banerjee A, Miller MT, Li K, et al. Towards a better diagnosis and treatment of Rett syndrome: a model synaptic disorder. Brain 2019; 142:239–248.

40. Moretti P, Levenson JM, Battaglia F, et al. Learning and memory and synaptic plasticity are impaired in a mouse model of Rett syndrome. J Neurosci 2006;26:319–327.

41. Morello N, Schina R, Pilotto F, et al. Loss of Mecp2 causes atypical synaptic and molecular plasticity of parvalbumin-expressing interneurons reflecting rett syndrome–like sensorimotor defects. eNeuro 2018;5: ENEURO.0086-18.2018.

42. Armstrong D, Dunn JK, Antalffy B, Trivedi R. Selective dendritic alterations in the cortex of rett syndrome. J Neuropathol Exp Neurol 1995;54:195–201.

43. Subramaniam B, Naidu S, Reiss AL. Neuroanatomy in Rett syndrome: cerebral cortex and posterior fossa. Neurology 1997;48:399–407.

44. Di Lazzaro V, Ziemann U. The contribution of transcranial magnetic stimulation in the functional evaluation of microcircuits in human motor cortex. Front Neural Circuits 2013;7:1–9.

45. Aberra AS, Wang B, Grill WM, Peterchev AV. Simulation of transcranial magnetic stimulation in head model with morphologically realistic cortical neurons. Brain Stimul 2020;13:175–189.

46. Ziemann U, Reis J, Schwenkreis P, et al. TMS and drugs revisited 2014. Clin Neurophysiol 2015;126:1847–1868.

47. Tsuboyama M, Lee Kaye H, Rotenberg A. Biomarkers obtained by transcranial magnetic stimulation of the motor cortex in epilepsy. Front Integr Neurosci 2019;13:57.

48. Suppa A, Huang YZ, Funke K, et al. Ten years of theta burst stimulation in humans: established knowledge, unknowns and prospects. Brain Stimul 2016;9:323–335.

49. Huang YZ, Edwards MJ, Rounis E, et al. Theta burst stimulation of the human motor cortex. Neuron 2005;45:201–206.

50. Castro J, Garcia RI, Kwok S, et al. Functional recovery with recombinant human IGF1 treatment in a mouse model of Rett Syndrome. Proc Natl Acad Sci U S A 2014;111:9941–9946.

51. Tropea D, Giacometti E, Wilson NR, et al. Partial reversal of Rett Syndrome-like symptoms in MeCP2 mutant mice. Proc Natl Acad Sci U S A 2009;106:2029–2034.

52. Pini G, Scusa MF, Congiu L, et al. IGF1 as a potential treatment for Rett syndrome: safety assessment in six Rett patients. Autism Res Treat 2012;2012:679801.

53. Pini G, Congiu L, Benincasa A, et al. Illness severity, social and cognitive ability, and EEG analysis of ten patients with Rett syndrome treated with mecasermin (recombinant human IGF-1). Autism Res Treat 2016;2016:5073078.

54. Khwaja OS, Ho E, Barnes KV, et al. Safety, pharmacokinetics, and preliminary assessment of efficacy of mecasermin (recombinant human IGF-1) for the treatment of Rett syndrome. Proc Natl Acad Sci U S A 2014;111:4596–4601.

55. Glaze DG, Neul JL, Kaufmann WE, et al. Double-blind, randomized, placebo-controlled study of trofinetide in pediatric Rett syndrome. Neurology 2019;92:e1912–e1925.

56. O'Leary HM, Kaufmann WE, Barnes K V., et al. Placebo-controlled crossover assessment of mecasermin for the treatment of Rett syndrome. Ann Clin Transl Neurol 2018;5:323–332.

57. Neul JL, Fang P, Barrish J, et al. Specific mutations in methyl-CpGbinding protein 2 confer different severity in Rett syndrome. Neurology 2008;70:1313–1321.

58. Downs J, Stahlhut M, Wong K, et al. Validating the Rett syndrome gross motor scale. PLoS One 2016;11:1–11.

59. Rossini PM, Burke D, Chen R, et al. Non-invasive electrical and magnetic stimulation of the brain, spinal cord, roots and peripheral nerves: basic principles and procedures for routine clinical and research application: an updated report from an I.F.C.N. Committee. Clin Neurophysiol 2015;126:1071–1107.

60. Chen R, Garg R. Facilitatory I wave interaction in proximal arm and lower limb muscle representations of the human motor cortex. J Neurophysiol 2000;83:1426–1434.

61. Kujirai T, Caramia MD, Rothwell JC, et al. Corticocortical inhibition in human motor cortex. J Physiol 1993;471:501–519.

62. Dubbioso R, Ranucci G, Esposito M, et al. Subclinical neurological involvement does not develop if Wilson's disease is treated early. Park Relat Disord 2016;24:15–19.

63. McDonnell MN, Orekhov Y, Ziemann U. The role of GABAB receptors in intracortical inhibition in the human motor cortex. Exp Brain Res 2006;173:86–93.

64. Nakamura H, Kitagawa H, Kawaguchi Y, Tsuji H. Intracortical facilitation and inhibition after transcranial magnetic stimulation in conscious humans. J Physiol 1997;498(Pt 3):817–823.

65. Dubbioso R, Raffin E, Karabanov A, et al. Centre-surround organization of fast sensorimotor integration in human motor hand area. Neuroimage 2017;158:37–47.

66. Wankerl K, Weise D, Gentner R, et al. L-type voltage-gated Ca2+ channels: a single molecular switch for long-term potentiation/long term depression-like plasticity and activity-dependent metaplasticity in humans. J Neurosci 2010;30:6197–6204.

67. Weise D, Mann J, Rumpf JJ, et al. Differential regulation of human paired associative stimulation-induced and theta-burst stimulation induced plasticity by L-type and T-type Ca2+ channels. Cereb Cortex 2017;27:4010–4021.

68. Rotenberg A. Measures of cortical excitability by transcranial magnetic stimulation. In: Inherited metabolic epilepsies. 2nd ed. New York, NY: Demos, 2018:201–206.

69. Ferguson BR, Gao WJ. Pv interneurons: critical regulators of E/I balance for prefrontal cortex-dependent behavior and psychiatric disorders. Front Neural Circuits 2018;12:37.

70. Eyre JA, O'Sullivan MC, Ramesh V, et al. Neurophysiological observations on corticospinal projections to the upper limb in subjects with Rett syndrome. J Neurol Neurosurg Psychiatry 1990;53: 874–879.

71. Nezu A, Kimura S, Takeshita S, Tanaka M. Characteristic response to transcranial magnetic stimulation in Rett syndrome. Electroencephalogr Clin Neurophysiol 1998;109:100–103.

72. Krajnc N, Zidar J. The role of transcranial magnetic stimulation in evaluation of motor cortex excitability in Rett syndrome. Eur J Paediatr Neurol 2016;20:597–603.

73. Asaka Y, Jugloff DGM, Zhang L, et al. Hippocampal synaptic plasticity is impaired in the Mecp2-null mouse model of Rett syndrome. Neurobiol Dis 2006;21:217–227.

74. Guy J, Gan J, Selfridge J, et al. Reversal of neurological defects in a mouse model of Rett syndrome. Science 2007;315:1143–1147.

75. Weng SM, McLeod F, Bailey MES, Cobb SR. Synaptic plasticity deficits in an experimental model of rett syndrome: long-term potentiation saturation and its pharmacological reversal. Neuroscience 2011; 180:314–321.

76. Li W, Xu X, Pozzo-Miller L. Excitatory synapses are stronger in the hippocampus of Rett syndrome mice due to altered synaptic trafficking of AMPA-type glutamate receptors. Proc Natl Acad Sci U S A 2016;113:E1575–1584.

77. Bachtiar V, Stagg CJ. The role of inhibition in human motor cortical plasticity. Neuroscience 2014;278:93–104.

78. Cárdenas-Morales L, Nowak DA, Kammer T, et al. Mechanisms and applications of theta-burst rTMS on the human motor cortex. Brain Topogr 2010;22:294–306.

79. Li CT, Huang YZ, Bai YM, et al. Critical role of glutamatergic and GABAergic neurotransmission in the central mechanisms of theta burst stimulation. Hum Brain Mapp 2019;40:2001–2009.

80. He LJ, Liu N, Cheng TL, et al. Conditional deletion of Mecp2 in parvalbumin-expressing GABAergic cells results in the absence of critical period plasticity. Nat Commun 2014;5:1–15.

81. Chao HT, Chen H, Samaco RC, et al. Dysfunction in GABA signalling mediates autism-like stereotypies and Rett syndrome phenotypes. Nature 2010;468:263–269.

82. Coghlan S, Horder J, Inkster B, et al. Neuroscience and biobehavioral reviews GABA system dysfunction in autism and related disorders: from synapse to symptoms. Neurosci Biobehav Rev 2012;36: 2044–2055.

83. Tarquinio DC, Hou W, Berg A, et al. Longitudinal course of epilepsy in Rett syndrome and related disorders. Brain 2017;140: 306–318.

84. Robinson L, Guy J, McKay L, et al. Morphological and functional reversal of phenotypes in a mouse model of Rett syndrome. Brain 2012;135:2699–2710.

85. Bernardo P, Cobb S, Coppola A, Tomasevic L, Di Lazzaro V, Bravaccio C, Manganelli F, Dubbioso R. Neurophysiological Signatures of Motor Impairment in Patients with Rett Syndrome. Ann Neurol. 2020 May;87(5):763-773.

86. Roche KJ, LeBlanc JJ, Levin AR, O'Leary HM, Baczewski LM, Nelson CA. Electroencephalographic spectral power as a marker of cortical function and disease severity in girls with Rett syndrome. J Neurodev Disord. 2019 Jul 31;11(1):15

87. Rucco R, Bernardo P, Lardone A, Baselice F, Pesoli M, Polverino A, Bravaccio C, Granata C, Mandolesi L, Sorrentino G, Sorrentino P. Neuronal Avalanches to Study the Coordination of Large-Scale Brain Activity: Application to Rett Syndrome. Front Psychol. 2020 Oct 27;11:550749.

88. Sorrentino, P., Rucco, R., Jacini, F., Trojsi, F., Lardone, A., Fabio, B., et al. . Brain functional networks become more connected as amyotrophic lateral sclerosis progresses: a source level magnetoencephalographic study. Neuroimage Clin. 2018; 20, 564–571.

89. Gross, J., Baillet, S., Barnes, G. R., Henson, R. N., Hillebrand, A., Jensen, O., et al. Good practice for conducting and reporting MEG research. Neuroimage 2013; 65, 349–363.

90. Polanía R, Nitsche MA, Ruff CC. Studying and modifying brain function with non-invasive brain stimulation. Nat Neurosci 2018;21:174–87.

91. Lefaucheur J-P, Antal A, Ayache SS, Benninger DH, Brunelin J, Cogiamanian F, et al. Evidence-based guidelines on the therapeutic use of transcranial direct current stimulation (tDCS). Clin Neurophysiol 2016;128:56–92.

92. Fabio RA, Gangemi A, Capri T, Budden S, Falzone A. Neurophysiological and cognitive effects of Transcranial Direct Current Stimulation in three girls with Rett Syndrome with chronic language impairments. Res Dev Disabil 2018;76:76–87.

93. Fabio RA, Gangemi A, Semino M, Vignoli A, Canevini MP, Priori A, et al. Effects of combined Transcranial direct current stimulation with cognitive training in girls with Rett syndrome. Brain Sci 2020;10:1–15.

94. Fonzo M, Sirico F, Corrado B. Evidence-based physical therapy for individuals with rett syndrome: A systematic review. Brain Sci 2020;10:1–20.